MISCELLANEOUS PAPER M-72-3

OPERATIONS AND MAINTENANCE MANUAL FOR A SCALE-MODEL LUNAR ROVING VEHICLE

by

A. S. Lessem

April 1972

Prepared for George C. Marshall Space Flight Center
National Aeronautics and Space Administration, Huntsville, Alabama

Conducted by Mobility and Environmental Division
U. S. Army Engineer Waterways Experiment Station, Vicksburg, Mississippi

Destroy this report when no longer needed. Do not return it to the originator.

The findings in this report are not to be construed as an official Department of the Army position unless so designated by other authorized documents.

MISCELLANEOUS PAPER M-72-3

OPERATIONS AND MAINTENANCE MANUAL FOR A SCALE-MODEL LUNAR ROVING VEHICLE

by

A. S. Lessem

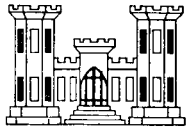

April 1972

Prepared for George C. Marshall Space Flight Center
National Aeronautics and Space Administration, Huntsville, Alabama

Conducted by Mobility and Environmental Division
U. S. Army Engineer Waterways Experiment Station, Vicksburg, Mississippi

ARMY-MRC VICKSBURG, MISS

FOREWORD

The study reported herein was conducted by personnel of the Mobility Research Branch (MRB), Mobility and Environmental (M&E) Division, U. S. Army Engineer Waterways Experiment Station (WES). The study was sponsored by the Apollo Program Office, National Aeronautics and Space Administration, Washington, D. C., and it was under the technical cognizance of Dr. N. C. Costes of the Space Sciences Laboratory, George C. Marshall Space Flight Center (MSFC), Huntsville, Ala. The work was performed under NASA - Defense Purchase Request No. H-72026A, "LRV Model Design, Fabrication, and Performance Study," dated 9 May 1970.

The study was conducted under the general supervision of Messrs. W. G. Shockley and S. J. Knight, Chief and Assistant Chief, respectively, of the M&E Division; and under the direct supervision of Dr. A. S. Lessem of the Research Projects Group, MRB, who also prepared this report.

COL Ernest D. Peixotto, CE, was Director of WES during the conduct of this study and preparation of this report. Mr. F. R. Brown was Technical Director.

CONTENTS

CONVERSION FACTORS, METRIC TO BRITISH AND BRITISH TO METRIC UNITS OF MEASUREMENT

Metric units of measurement used in this report can be converted to British units as follows:

Multiply	By	To Obtain
centimeters	0.3937	inches
meters	3.2808	feet
grams	0.0022	pounds (mass)
newtons	0.2248	pounds (force)
meter-newtons	0.7375	foot-pounds
meganewtons per cubic meter	3.684	pounds per cubic inch

British units of measurements used in this report can be converted to metric units as follows:

Multiply	By	To Obtain
pounds (force)	4.4482	newtons

SUMMARY

A one-sixth scale model of the Lunar Roving Vehicle used in the Apollo 15 mission was built and instrumented to conduct model studies of vehicle mobility. The model was free running under radio control and was equipped with a lightweight telemetry transmitter that allowed 16 channels of data to be gathered simultaneously. String payout and fifth-wheel devices were developed to measure vehicle velocity. Other real-time measurements included wheel torque, wheel speed, center-of-gravity accelerations, and steering forces. Calibration, operations, and maintenance procedures were worked out.

Details of the development of the instrumentation, its maintenance, some of the problems encountered, etc., are recorded in this report to serve as a preliminary operations and maintenance manual for this specific model. In addition, information regarding soil processing and testing that may be useful to NASA personnel planning mobility research with the model in soil is furnished.

OPERATIONS AND MAINTENANCE MANUAL FOR A SCALE-MODEL LUNAR ROVING VEHICLE

PART I: INTRODUCTION

Background

1. The use of scale models is an attractive tool of design and analysis, especially in cases where it is impossible or impractical to deal with full-scale prototypes. Scale modeling is a well-established practice in aerodynamics and hydrodynamics studies, but has seen less success in studies of land vehicles. One important reason for this state of affairs is that soil is a much more complex environment than are air and water and has proven difficult to study in terms of modeling theory.* Another reason is that a small-size model vehicle must support a scaled load, which, when made up of transducers and support electronics, allows relatively few measurements on board before the weight limit is attained. In addition, the use of umbilical cords for transmission of power and signals has heretofore been necessary, with inevitable restrictions on vehicle dynamics and maneuvering. These factors, together with vehicle prototype costs significantly less than those of aircraft and ships, have not encouraged wide application of model theory to soil-vehicle systems. However, prototype costs of military, agricultural, and commercial vehicles continue to increase, not to mention those of special-purpose vehicles such as the lunar rover. As a result, continued

---

* D. R. Freitag, R. L. Schafer, and R. D. Wismer, "Similitude Studies of Soil-Machine Systems," Journal of Terramechanics, Vol 7, No. 2, 1970, pp 25-59.

development of soil-vehicle scale models is necessary to provide increasing support for rational vehicle design.

Purpose

2. The purpose of this study was to develop instrumentation, maintenance, and operations procedures for a specific small-scale model of the lunar roving vehicle (LRV) as configured for the Apollo 15 mission. The principal purpose of this report is to serve as a first-generation operations and maintenance manual for National Aeronautics and Space Agency (NASA) personnel who plan to conduct tests with the model. In addition, the report contains information concerning soil processing and testing.

Scope

3. A one-sixth scale, radio-controlled model of the Apollo 15 LRV was constructed and instrumented with lightweight transducers. A lightweight, small-size telemetry transmitter was obtained, allowing development of an umbilical-free measurement system. Low-drag string payout and fifth-wheel devices also were developed. Tests were conducted to work out effective operating and maintenance procedures.

PART II: THE VEHICLE, INSTRUMENTATION, AND MAINTENANCE

The Vehicle

4. The scale-model LRV (fig. 1) is 51 cm* long and 34 cm wide. The geometric scale is one-sixth that of the actual vehicle. The main features of the suspension, steering, and wheels were geometrically scaled from the prototype vehicle. The wire-mesh wheels of the prototype were simulated on the model by a woven nylon mesh. The only significant departure from proper geometric scaling was the use of hull-mounted motors on the model instead of hub-mounted motors as on the prototype.

5. The scaling laws for the model are outlined in Appendix A, and result in a total weight of approximately 31 N. Of this total, the model, batteries, and radio control components weigh 20 N, leaving 11 N for all instrumentation. This weight limitation was met by using very lightweight components and by devising measurements requiring little additional structural weight. It should be noted, also, that the control and instrumentation components are glued in place and are capable of being relocated to allow changes in distribution of weight if desired.

6. The key mechanical elements in the model are the drive shaft, wheel bearings, and wheels. Each drive shaft is made up of two universal joints and a spline. Torque is transmitted to the wheels through the entire ranges of suspension flexure and steering angles. The transmission of torque, however, is not entirely smooth, but fluctuates cyclically as

---

* A table of factors for converting metric to British and British to metric units of measurement is given on page ix.

the drive shaft rotates. The wheel "bearing" consists of two concentric brass sleeves with dry lubricant between them. Although the bearing is of a rather rudimentary design, it has performed satisfactorily, presenting fewer maintenance problems than anticipated. The wheels were handmade from a rewoven nylon mesh epoxied to an aluminum hub. Inevitably, the wheels were somewhat out-of-round and distorted; however, they were within acceptable dimensional limits. With the instrumentation configured as shown in fig. 1b, the static deflected radii and the average effective radii* of the wheels were as shown on page 5. These were averages of measurements taken at four equally spaced points on each wheel; the wheel was rotated so that each point, in turn, underwent deflection. The wheel load in each case was approximately 7.7 N, corresponding to the wheel load of the prototype on the moon divided by 36 (see Appendix A).

Instrumentation

7. The instrumentation system consists of assorted transducers whose signals are telemetered to a remote data-gathering station. The system is completely self-contained and has a total weight consistent with the scaled loading of the actual LRV. The key element is the telemetry transmitter package whose characteristics are tabulated below.

Number of data channels: 16

Sample rate per channel: 200/sec

---

* A. J. Green, "Performance of Soils Under Tire Loads; Development and Evaluation of Mobility Numbers for Coarse-Grained Soils," Technical Report No. 3-666, Report No. 5, Jul 1967, U. S. Army Engineer Waterways Experiment Station, CE, Vicksburg, Miss.

A. J. Green and K.-J. Melzer, "Performance of the Boeing LRV Wheels in a Lunar Soil Simulant; Effects of Wheel Design and Soil" (in preparation), U. S. Army Engineer Waterways Experiment Station, CE, Vicksburg, Miss.

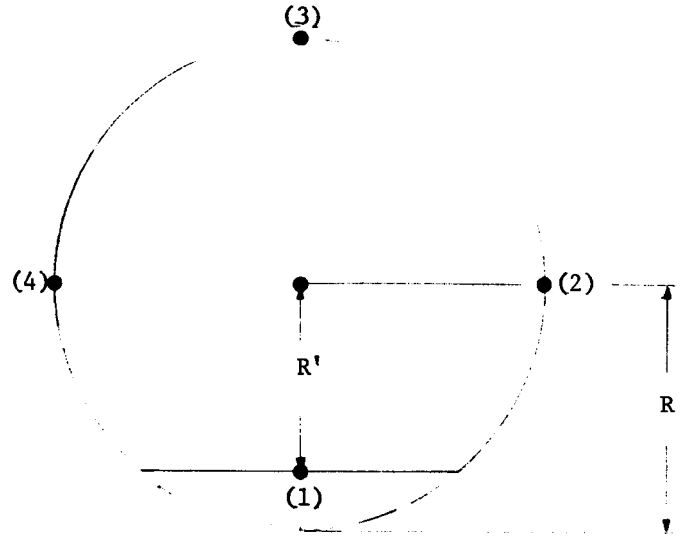

Wheel No.	Point	Undeflected Radius R, cm	Deflected Radius R', cm	Deflection δ, cm	Effective Radius R_e, cm*	Average Effective Radius, cm
1	1	6.553	6.032	0.521	6.293	6.314
	2	6.555	6.058	0.487	6.312	
	3	6.563	6.091	0.472	6.327	
	4	6.558	5.994	0.464	6.326	
2	1	6.502	6.058	0.444	6.280	6.318
	2	6.565	6.147	0.419	6.355	
	3	6.515	6.071	0.444	6.293	
	4	6.558	6.134	0.424	6.346	
3	1	6.439	5.949	0.490	6.194	6.265
	2	6.566	6.147	0.419	6.356	
	3	6.492	6.119	0.373	6.305	
	4	6.452	5.956	0.496	6.204	
4	1	6.627	6.223	0.404	6.425	6.517
	2	6.731	6.284	0.447	6.508	
	3	6.794	6.411	0.383	6.603	
	4	6.789	6.274	0.515	6.532	

* $R_e = \frac{R + (R - \delta)}{2}$

Weight with battery: 5.27 newtons

Size: 15.2 by 12.7 by 5.1 cm

Carrier frequency: 88-108 MHz

Range: 16 m

Operation time per battery charge: 30 min

Data from the transducers are multiplexed onto a single FM carrier and decoded into separate simultaneously available analog data channels at the receiver. At this point, the data can be recorded on magnetic tape or displayed on oscillographs as desired. The light weight, small size, and channel capacity of the transmitter made the development of the measurement system possible. The transmitter was designed and built by Inmet Corporation, Indian Harbour Beach, Florida, and was the first such unit fabricated by the manufacturer. In addition to general-purpose tape recorders and oscillographs, the instrumentation required for gathering data from the model is shown in fig. 2. A schematic diagram of the oscillograph/tape recorder panel is shown in fig. 3.

Measurements

8. Motor current is determined separately for each of the four wheel motors by monitoring the voltage developed across a precision 0.1-ohm resistance in which the motor current is flowing. The location of this resistance in the motor circuitry is indicated in fig. 4. Note that current flows in the same direction in the resistance regardless of the direction of motor rotation, Thus, a voltage of positive polarity is normally produced in proportion to the magnitude of current without regard to direction of rotation. This voltage is applied to a telemetry channel having an input range of 0.1 v (corresponding to a current range of 1 amp).

Each telemetry channel has a zero-offset control that allows the location of the zero of voltage to be set at will throughout the input range. The initial setup of this control places the zero of voltage in the center of the range, which means that each motor current is measured in the range of -0.5 to +0.5 amp. This setup was made in anticipation of the desire to register the overrunning of the motors by the vehicle on downhill slopes. Experience with the vehicle will suggest optimum location of zeros.

9. Motor voltage is measured by using a voltage divider attached to the main power buss, as shown in fig. 4. The voltage applied to all motors is the same and is recorded by a single telemetry channel. This channel has been zero-centered and has an input range of -5 to +5 v. The zero-centering in this instance can be altered if more resolution is required as suggested by experience with the vehicle.

10. Wheel speed is determined from a time history of pulses, wherein the time between adjacent pulse peaks is the time for one revolution of the wheel. These pulses are obtained by using a voltage divider, as shown in fig. 5, one element of which is a light-sensitive resistance oriented to sense light reflected from the motor drive shaft. Half the surface on the circumference of the drive shaft is dull black; the other half is bright. Ambient light is used, producing pulses of varying height; however, the peak-to-peak spacing of the pulses remains apparent. The speed of each wheel is measured in this way. Four telemetry channels, each zero-centered in a range from -5 to +5 v, are assigned to this measurement.

11. Vehicle attitude is determined by using two accelerometers with their sensitive axes positioned horizontally in the transverse and longitudinal directions. The offsets of these accelerometers are proportional to the sines of the angles formed by their sensitive axes with the horizontal space-fixed coordinate plane. The determination of these two angles fixes the inclination of the plane of the vehicle bed with the horizontal. Note that the plane of the vehicle bed could be rotated about a vertical axis with no changes in the accelerometer offsets. Thus, the measurement gives vehicle inclination without reference to direction of motion. Note also that the determination of attitude is best accomplished with the vehicle at rest so that there is no contribution by dynamics to the registration of the accelerometers. Two telemetry channels, zero-centered in a range of -5 to +5 v, are assigned to this measurement.

12. Vertical acceleration is measured by an accelerometer with its sensitive axis perpendicular to the plane of the vehicle bed. This accelerometer, together with those whose offsets measure vehicle attitude, make up an orthogonal array registering acceleration dynamics along the body-centered pitch, roll, and yaw axes of the vehicle. One telemetry channel, zero-centered in a range of -5 to +5 v, is assigned to this measurement. However, for steady state operations where vertical dynamics are not of interest, this data channel is assigned to another measurement.

13. Steering force is measured by strain gages mounted on the steering links (fig. 1c). Because of the small surfaces available for the strain measurement, semiconductor gages of high sensitivity had to be used. These gages are subject to significant temperature effects and are

critically dependent upon correct emplacement. These factors, together with considerable scraping and friction within the steering assembly, render the measurement of steering forces troublesome. The electrical setup is depicted in fig. 6. Note that each bridge of gages has its own tailor-made circuitry, reflecting the sensitivity of these gages to the circumstances of their mounting. In addition, the location of the sensitivity resistors for each gage in the cluster of resistors mounted on the vehicle is shown. Four telemetry channels, especially arranged for strain transducers, are assigned to this measurement.

14. Vehicle speed and elapsed distance for straight-line runs are measured by the string payout device illustrated in fig. 7a, in which the device is arranged on a table top for clarity. Four pulleys support a string attached to the front and the rear of the vehicle. The string drives a slotted circular plate mounted on one of the pulley supports. The slots, sensed by a lamp and photocell, produce pulses whose separation in time is proportional to vehicle velocity. The apparatus exerts negligible drag on the vehicle. No use of telemetry is required for this measurement; a cable carries signals directly to the data-collection panel.

15. Vehicle speed and elapsed distance for maneuvered runs are measured by the fifth-wheel device illustrated in fig. 7b. As a towed wheel, the device is subject to a small amount of slipping. This has been reduced as much as possible by using sealed bearings with dry lubricant and grousers. Nevertheless, slip remains an important factor, with the fifth wheel registering from 94 to 98 percent of the vehicle speed as

reported by the string payout device. This problem is discussed in paragraph 43. As in the case of the wheel speed measurement, a photocell senses the passage of alternating light and dark surfaces and produces pulses correlated with the rotational speed of the fifth wheel.

16. Drawbar pull. A lightweight proving-ring load cell was obtained for use with the string payout device. As of July 1971, the load cell had not been installed. The most direct method of measuring drawbar pull is to attach this load cell directly to the vehicle, attach the payout string to the load cell, and install a friction snubber on one of the pulleys. The load cell will register drawbar pull directly. One strain channel of telemetry will be required for transmission of data at the expense of one of the steering force measurements.

Channel assignments

17. Telemetry channel assignments are as follows:

Telemetry Channel	Measurement
0	Current/torque, motor 1
1	Current/torque, motor 2
2	Current/torque, motor 3
3	Current/torque, motor 4
4	Wheel speed, motor 1
5	Wheel speed, motor 2
6	Wheel speed, motor 3
7	Wheel speed, motor 4
8	Longitudinal acceleration
9	Transverse acceleration
10	Vertical acceleration, or fifth-wheel speed, or string payout signal
11	Motor voltage
12	Steering force, wheel 1

Telemetry Channel	Measurement
13	Steering force, wheel 2
14	Steering force, wheel 3
15	Steering force, wheel 4

Calibrations

18. Motor current is calibrated as indicated in fig. 6. The basic idea is to inject a known current into the precision 0.1-ohm measurement resistor and monitor the corresponding telemetered output. The following procedure is specific for motor 1; similar procedures pertain to the other motors.

19. To inject a known current into the measurement resistor of motor 1, switches A and B (fig. 4) must be put into their normally open states. This can be accomplished by inserting small wedges between the switch rollers and the cam. A laboratory power supply, a series current-limiting resistance, and a precision 1-ohm resistance are arranged in a series circuit with the 0.1-ohm measurement resistor as shown in fig. 8. The telemetry receiver is allowed to warm up for 30 minutes and the telemetry transmitter for about 5 minutes, and channel 0 is monitored. The power supply is then adjusted to provide a sequence of known currents, as determined by the voltage across the 1-ohm resistance, and the corresponding telemetry receiver output voltage is recorded. A plot of these output voltages versus input currents calibrates this measurement. Plots for channels 0-3 are given in fig. 9.

20. Torque is calibrated by applying known torques to the drive shaft and measuring the corresponding motor current. The calibration setup is shown in fig 10. The procedure is as follows:

a. Mount the vehicle in the calibration jig and tighten clamps.

b. Remove the wheel and clean the brass tubing bearings, and apply fresh graphite lubricant.

c. Replace the wheel, and mount the torque cylinder (with weight basket removed) to the hub. Adjust the wheel position so that the torque cylinder is horizontal. Using a laboratory power supply in place of the vehicle batteries, run the wheel motor at its slowest speed, and record the current. Note that the presence of the universal joints results in a somewhat fluctuating current, which should be recorded on a strip chart so that an average value can be obtained.

d. Fasten the weight basket to the torque assembly, and mount weights. Run the motor at its slowest speed to allow the weight basket to wind uniformly on the cylinder and record the current.

Torque calibration curves produced in this manner are shown in fig. 11. The weights used correspond to masses of 100, 200, 300, and 400 grams in a basket whose weight corresponds to a mass of 20.7 grams. The radius of the torque cylinder is 3.81 cm. The basic torque equation is:

$$T_0 = \Delta T = K(I_0 + \Delta I) \qquad (1)$$

where

T_0 = reaction torque in wheel bearing with torque cylinder mounted.

ΔT = incremental torques added by weights in weight basket.

I_0 = motor current corresponding to T_0.

ΔI = corresponding incremental currents

Equation 1 can be written as the sum of the following equations:

$$T_0 = KI_0$$

$$\Delta T = K\Delta I$$

A value of K can be ascertained by plotting ΔT versus ΔI and fitting a straight line to the plot. Then, total torque can be computed by using total current $(I + \Delta I)$.

21. An alternative procedure is to telemeter the current measurement, and calibrate the receiver output directly in terms of the applied torque. A sample calibration is shown in fig. 12, and the "end-to-end" calibrations of the four motors are given in fig. 13. Note that these will be somewhat different from similar graphs based on the torque-current and current-voltage calibrations, because the torque available at the drive shaft is dependent on the state of maintenance of the wheel bearings. Torque calibrations taken at different times will not be quite the same.

22. Motor voltage is calibrated by applying a known voltage to the measurement potentiometer (fig. 10) and adjusting it for the desired corresponding output at the telemetry receiver. For example, as presently set up, 25 v applied to the drive motors produces 5 v at the receiver.

23. Wheel speed requires no calibration.

24. Vehicle attitude is calibrated by putting the vehicle in any convenient fixture whose attitude can be controlled separately in pitch and roll. Plots of telemetry output versus angle are illustrated in fig. 14.

25. Vertical acceleration is calibrated by a 1-g offset that appears upon application of power to the accelerometer.

25. Steering force is calibrated by applying known forces to the steering link on which the strain gages are mounted. The steering link must be removed from the vehicle; electrical connections are maintained through a test cable, as shown in fig. 15. The steering link is placed in a test jig (for example, a vise with smooth jaws), and tensile and compressive forces are applied by suspending known weights while corresponding telemetry voltages are recorded. Calibration curves for this measurement are given in fig. 16. Note that the tie rod should be removed, and the steering link clamped, as shown in fig. 17.

27. Vehicle speed and elapsed distance measured by using the string payout device require no calibration. The size of the slotted disk is arranged so that two successive pulses correspond to traversal of 7.62 cm.

28. Vehicle speed and elapsed distance measured by using the fifth wheel require no calibration. Two successive pulses correspond to one-half revolution of the fifth wheel. The radius of the wheel is 5.84 cm.

Maintenance

29. The only mechanical items requiring periodic maintenance are the universal joints and the wheel bearings. Because of their small size and the considerable torque they must transmit, the universal joints frequently failed by shearing and distortion of the pivot pins. This is a materials problem that can be solved by using harder pins; until this is done, a supply of spare universal joints must be maintained. It should

be noted that the set screws in the universal joints tend to work loose under high torque loads and should be checked frequently for tightness.

30. Although they are unprotected by dust seals, the wheel bearings have proven to be quite tolerant of the dusty environment presented by operations on the lunar soil simulant. Nevertheless, the wheels must be removed periodically and the bearings cleaned. A dry graphite lubricant should be used when they are reassembled. It is imperative that this be done prior to calibrating the torque measurement. During normal operations, carefully blowing out the bearings with high pressure air following each test and determining that the bearings remain free and loose will suffice. Any sign of binding is an indication that the bearings should be cleaned. If trouble is experienced as the bearings continue to wear, it may be wise to consider the use of nylon or teflon facings for the bearing surfaces.

PART III: SOIL PROCESSING AND TESTING

31. The lunar soil simulant (LSS) used with the scale-model LRV has been described in detail by Green* and Melzer.** Briefly, it is a crushed basalt with a grain-size distribution approximating those of the Apollo 12-15 soil samples. The soil condition desired for testing, termed LSS_4, had an average cone penetration resistance gradient G of 1.03 MN/m^3.

32. In view of the amount of soil and the types of test bins available, it was decided to separate the tests according to whether steady-state or transient conditions were being studied. A soil bin 163 cm wide and 7 m long was used for steady-state tests, in which straight-line runs were of interest. A second bin approximately 2 m long and 3 m wide was used for tests in which maneuvering and dynamics were important. In both bins, the soil was placed to a depth of about 13 cm overlying a plywood base, in turn overlying a sand filler of sufficient quantity to bring the soil surface to within 10 cm of the top of the bin. It is important, especially in the case of the maneuver tests, to have a barrier around the testing area so that the vehicle cannot fall off the test bin. This was most easily accomplished by keeping the soil surface somewhat below the top edge of the test bin.

---

* A. J. Green and K.-J. Melzer, "Performance of Boeing-GM Wheels in a Lunar Soil Simulant (Basalt)," Technical Report M-70-15, Oct 1970, U. S. Army Engineer Waterways Experiment Station, CE, Vicksburg, Miss.

** K.-J. Melzer and A. J. Green, "Performance Evaluation of a First-Generation Elastic Loop Mobility System," Technical Report M-71-1, May 1971, U. S. Army Engineer Waterways Experiment Station, CE, Vicksburg, Miss.

33. To prepare the LSS_4 condition, enough water was thoroughly mixed into the soil to bring the moisture content to approximately 1.8 percent. The soil surface was covered when not in use and occasionally sprayed to compensate for evaporation. Soil processing consisted of plowing with a seed fork to the total soil depth of 13 cm and compacting with a vibrator until the desired density was obtained. Note, however, that the screeding process used by Green and Melzer was abandoned in this study; there was no further processing following compaction. Because wheel sinkages of just a few centimeters are encountered, the model is very sensitive to the state of the soil surface, and the density of the soil at the surface is adversely affected by the screeding process, especially when accomplished by hand-held screed boards. However, the main purpose of screeding, the leveling of the soil surface, was not accomplished, and the soil section following compaction was somewhat irregular.

34. The soil processing methods worked out within available time and funds were not entirely satisfactory. They are essentially applications of satisfactory methods worked out by Green and Melzer for bin-emplaced soil traversed by full-size wheels. For model studies where surface effects predominate, considerable refinement of processing techniques will be required. The most pressing problem is the nonuniformity of the soil density throughout the test area. This problem was troublesome in the long soil bins, where the width of the test lane corresponded to the width of the vibrator. It was especially troublesome in the wider bin in which maneuver tests were conducted, where the width of the test lane corresponded to several adjacent widths of the vibrator. In this

case, the compaction of one part of the surface by the vibrator was upset when the adjacent area was processed. It is apparent that processing of soil masses of surface area sufficient for studing the performance of free-running scale models will require the development of special tools and techniques.*

35. Because of its capability for measuring surface soil strength, a "multi-probe" cone penetrometer (fig. 18) was used to test soil strength, for adequate compaction. The penetrometer was used in conjunction with a strip chart recorder to produce a force-penetration curve from which the average penetration resistance gradient G was determined.

---

* Note added in proof: NASA personnel have determined that satisfactory compaction and uniformity of density can be attained by building up the soil mass in thin layers. The layers are approximately 2.5 cm thick and are separately compacted with a weighted roller prior to deposition of the next layer. The total height of the soil mass so constructed is approximately 16 cm on level surfaces and somewhat higher where obstacles are constructed.

PART IV: OPERATIONS

Normal Mode Operations

36. Separation of tests according to whether steady-state or maneuver conditions were to be studied proved convenient. Steady-state tests involve straight-line runs over a soil surface of sufficient length to allow several seconds of vehicle operation at constant speed. Maneuver tests involve changing the direction of the vehicle, a circumstance that seldom allows a steady state to be attained.

37. The only difference in the setup of equipment for steady-state and maneuver tests is that the string payout device is used in the former, and the fifth wheel in the latter. In theory, the fifth wheel can be used exclusively; however, until more experience is gained with its use in computing slip, use of the string payout device where possible is considered wise.

38. Normal mode operations refer to tests of the vehicle in which all functional components operate as intended. Test setup procedures are as follows:

a. Prepare soil test section. Note that for straight-line tests, several tests can be run side-by-side in the same test section. For maneuver tests, a fresh test section will be required for each test.

b. Allow warmup of data recording instruments. Place the telemetry antenna (fig. 2) as close as possible to the test area.

c. Attach velocity measuring device, and place model on test section. If a straight-line test is to be conducted, the string payout device is used; if a maneuver test, the fifth wheel is used. Note that the string payout device has its own signal cable and does not use telemetry; the fifth wheel uses telemetry. As presently set up, the vertical acceleration channel is sacrificed whenever either velocity measuring device is used. A front-panel switch on the oscillograph panel allows oscillograph channel 10 to be connected to either the string payout signal or the signal from telemetry channel 9, to which either the vertical accelerometer or the fifth-wheel speed sensor is attached.

d. Arrange for angular orientation of test bin. When testing of the vehicle on sloped surfaces is desired, it is necessary to orient the test bin to provide the proper slope angles. This is accomplished most easily and safely with an overhead crane.

e. Calibrate with telemetry OFF. This involves switching +5 and -5 v to the oscillograph galvanometers, using the front-panel switch on the oscillograph/tape recorder panel. These voltages represent the maximum signal excursions to come from the telemetry receiver. This calibration must be accomplished first with telemetry transmitter and receiver OFF, so that proper zeros can be read on the motor voltage and vertical acceleration channels (with telemetry ON, these channels have normal offsets).

f. Switch on telemetry and power supplies on vehicle. Allow 3 minutes for telemetry warmup. Also, switch on the radio control receiver. The power supplies referred to are those for propulsion, wheel speed sensors, and accelerometers. Make sure that the direction-control servo on the vehicle is in its neutral position (no vehicle motion).

g. Calibrate with telemetry ON. Follow procedures in e above, except telemetry transmitter and receiver are ON.

h. Operate vehicle. Switch on radio control transmitter, place oscillograph and tape recorder (if used) in operation, and conduct test.

i. Secure vehicle. Following the test, switch off all power supplies, telemetry, and radio control components. Place vehicle on the torque calibration test jig for safekeeping and to keep vehicle weight off the wheels. If the vehicle is to be idle for several hours, place wheel covers on the wheels to maintain their shape. Recharging propulsion and transmitter batteries (both telemetry and radio control) between tests is a good practice.

Degraded Mode Operations

39. Degraded mode operations are intended to simulate failures of various mecnanical and electrical components on the vehicle and to ascertain performance penalties. Test setups and procedures are identical

to those for normal mode operations, except for modifications to the vehicle corresponding to specific cases of interest to NASA personnel, as follows:

a. Failure of motors in locked condition. Failure of the motors in a locked condition can be simulated by disconnecting the power plugs to the desired motors.

b. Freewheeling of wheels. Freewheeling can be simulated by removing the spline and lower drive shaft on the desired wheels.

c. Failure of motors in backdrive condition. This condition cannot be simulated on the model vehicle.

d. Steering motor lock. Steering motor lock can be simulated by switch control of fore and aft steering servos. This control is installed on the vehicle.

e. Steering motor disconnected. Disconnection of the steering motor can be simulated by removing the steering servo. The steering gear will then be free to slew from side to side.

f. Wheel failure. Wheel failure can be simulated by deforming the model wheels as desired and securing the deformation with fine wires attached to the nylon mesh of the wheels.

PART V: SUMMARY OF EXPERIENCES

40. The following discussion bears on a variety of topics reflecting accumulated experience in working with the scale-model LRV.

Problems with Torque Measurements

Error in analysis of torque meausrement

41. As mentioned earlier, the calibration of the torque measurement depends on the state of maintenance of the wheel bearing. To illustrate this fact, torque calibrations for the four wheels taken at different times are illustrated in figs. 19a-19d. These calibration curves are all superimposed in fig. 19e to give an overall idea of the spread in the measurements. The outcomes of calibration trials under different conditions of temperature and dust environment are shown in fig. 20. It is apparent that refinement of the wheel bearing and drive shaft linkages will be required to eliminate mechanically induced fluctuations in torque delivered to the wheels.

Extension of torque calibrations

42. As discussed earlier, the torque measurement is calibrated in the range of motor currents from zero to 0.5 amp. All level-surface maneuvering by the vehicle on rough or smooth surfaces is accomplished with motor currents of less than 0.5 amp. However, when the vehicle is operated on slopes, especially under stalled conditions, the motor currents exceed 0.5 amp and are thus beyond the range of the torque calibration. Although extension of the calibration would be desirable,

it would be difficult to do so by using the procedure described earlier, in which known forces act through known distances in the form of suspended weights winding up on a torque cylinder mounted on a rotating wheel. The difficulty arises because heavy suspended weights introduce serious extraneous forces when they are accelerated from rest or are inadvertently jarred. The forces are of sufficient magnitude to disrupt the calibration and to overstress the drive shafts. Alternate methods for torque measurement involve the design of a special-purpose dynamometer. However, satisfactory torque measurements can possibly be obtained by simply extending the straight line of each existing torque calibration.

Problems with Slip Measurement

43. In terms of reporting absolute values of vehicle translational velocity, the fifth-wheel device closely matches the string payout device as shown by tests conducted to compare the two devices. However, when these values are combined with values of wheel speeds to compute slips, significant differences appear when string payout and fifth-wheel velocities are used because the slip formula is based on velocity differences. Of the two devices, the string payout is more accurate, but it is limited to use in straight-line tests. The fifth-wheel device is less accurate, but it can be used in free-run maneuver tests. The use of photography is, as discussed below, an impractical alternate. Thus, there seems to be no recourse available other than to conduct tests comparing the string payout and fifth-wheel devices, so that a correction procedure can be worked out for application to fifth-wheel readings.

Problems with Photography

44. Photography is often considered for use in determining slip and absolute vehicle velocity, and offers an attractive solution to the problem of their accurate determination. However, because of the difficulty of maintaining proper alignment of the camera and vehicle and the laborious processing of pictures to extract the desired data, photography is not a useful procedure except for checking or calibrating other devices, or for handling short data runs. For cases where slip and speed are to be measured continuously throughout tests of duration greater than just a few seconds, the use of photography creates more problems than it solves.

Out-of-Round Wheels

45. The gathering of data for slip computations will be plagued by out-of-round wheels even if it is perfect in all other respects. The rolling radius used in slip computation is not constant either during the course of a test or from test to test. Measurements of average rolling radius are dependent on the usage history of the vehicle. As mentioned earlier, the vehicle should not be permitted to rest on its wheels between tests, and should be stored with the wheel covers in place during idle periods.

Maneuver Area

46. The soil bin used for maneuver tests was just large enough to permit the vehicle to drive through one complete turning circle. A

larger maneuver area should be used to free the operator from concern about impacting the side of the bin and to allow ample traversal of virgin soil surface during random maneuvering operations. An area of about 7 m by 7 m would be desirable.

Improvement of Wheel Speed Measurement

47. The arrangement for the wheel speed measurement, intended to minimize weight and power requirements, involves pickup of reflected ambient light by a photocell from bright portions of the drive axle. The test area must be strongly illuminated because the bright area sensed by the photocell is small. For straight-line tests, in which the orientation of photocells and light sources was relatively constant, this method produced satisfactory results. However, photocell registration was disrupted during maneuver tests when the vehicle was oriented so that the photocells could pick up direct rays from the light source. On some occasions, the telemetry channel was saturated by this occurrence, and the measurement was disrupted until the vehicle orientation changed. At the inevitable expense of added weight, the wheel speed measurement should be made independent of reflected light.

Alteration of Telemetry Channel Zero Settings

48. Because of the lead time required to fabricate the telemetry equipment, channel ranges and zero settings had to be specified in advance of the construction of the vehicle and the arrangements for data measurements. The decision was made to center the zeros in the middle

of the ranges of all channels. For example, motor currents would be measured over a range of 1.0 amp from -0.5 to +0.5 amp. Although they are generally satisfactory, some of the measurements did not take full advantage of the dynamic range of their telemetry channels. For example, the wheel speed pulses are of one polarity and vary over no more than one half of the available range. More seriously, this is true also of the motor current measurements, which have shown saturation of their telemetry channels under conditions of high-throttle slope climbing. The zero setting of each channel can be altered as follows: In the telemetry receiver, there is a wire jumper adjacent to the gain adjust potentiometer for each channel. This jumper must be removed. In the telemetry transmitter, there is an offset control for each channel. This control can be reset to place the measurement zero as desired within the dynamic range. For example, it would be desirable to measure motor currents from 0 to +1.0 amp, or perhaps from -0.1 to +0.9 amp. Note that the front-panel monitoring meter on the receiver is intended for centered-zero channels and will be overranged when monitoring channels in which the zero is positioned at one side. Another meter should be used in that case.

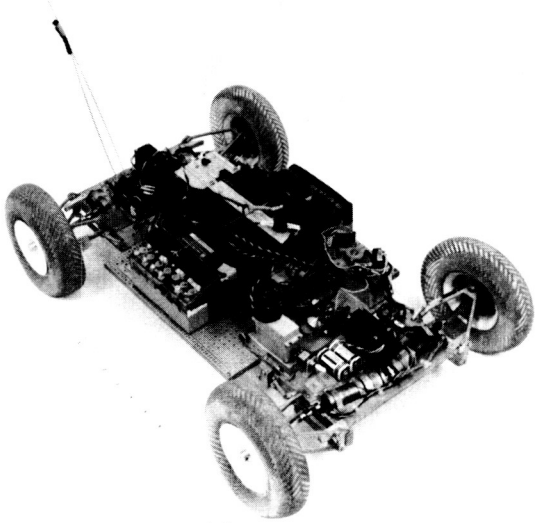

a. Overall view

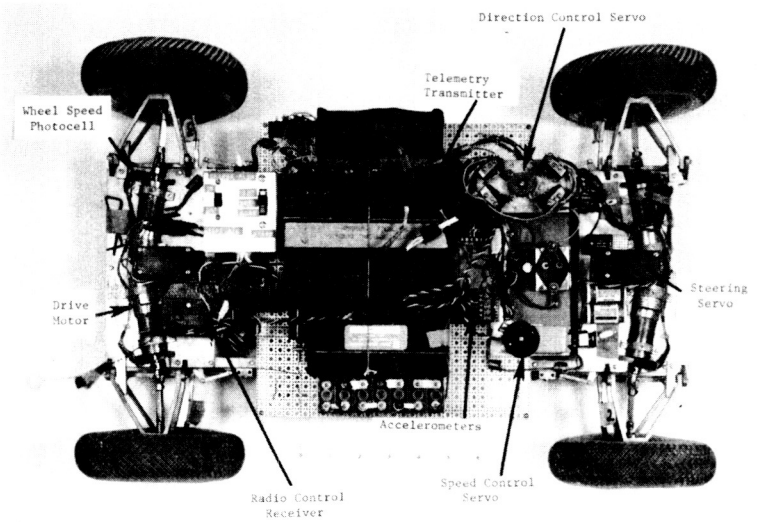

b. Parts layout viewed from above

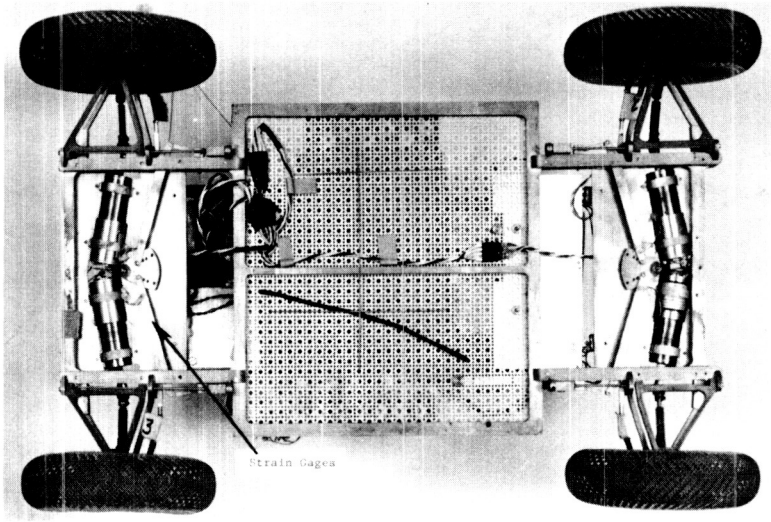

c. Parts layout viewed from below

Fig. 1. Scale-model Lunar Roving Vehicle (LRV)

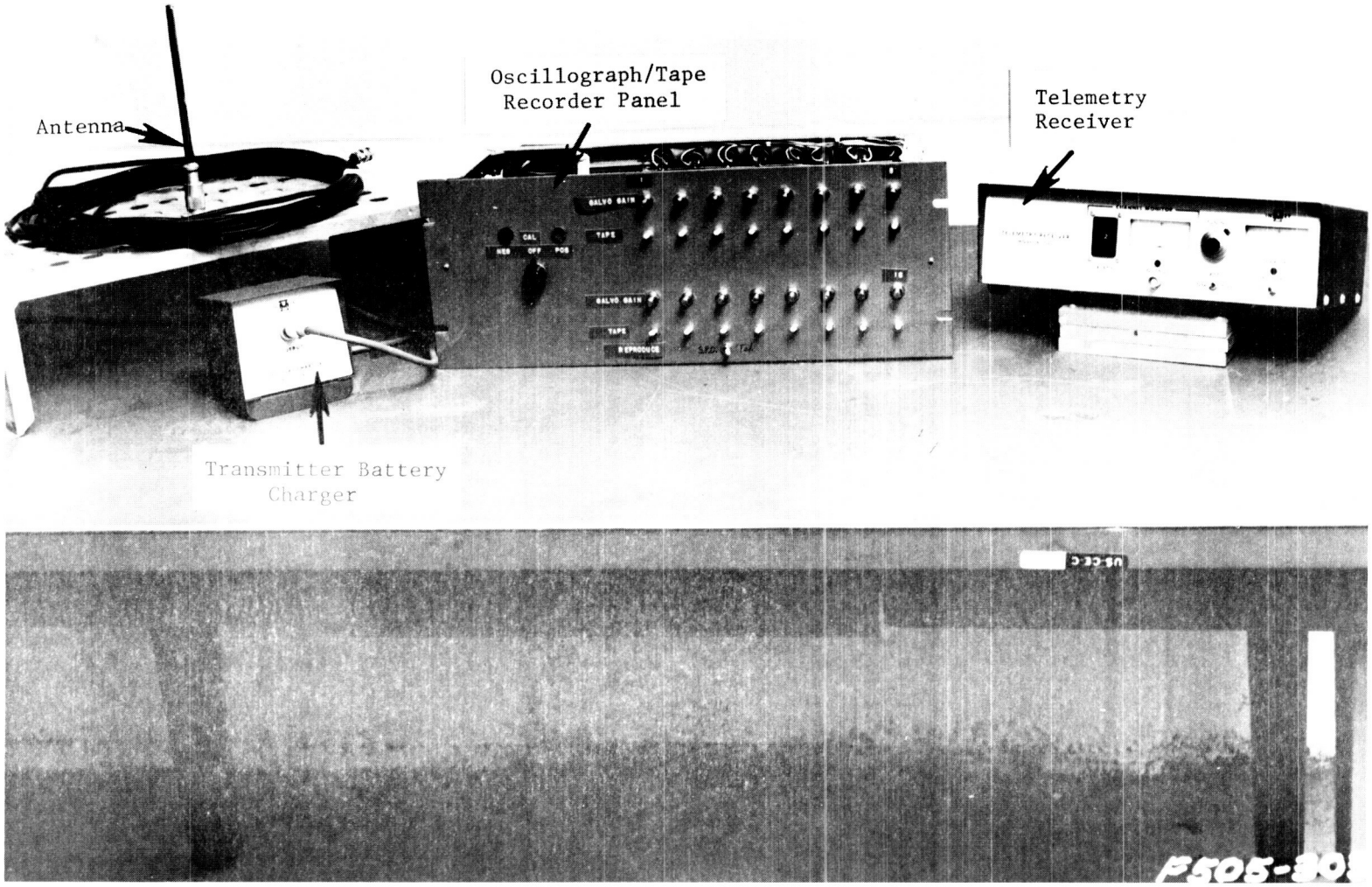

Fig. 2. Telemetry instrumentation

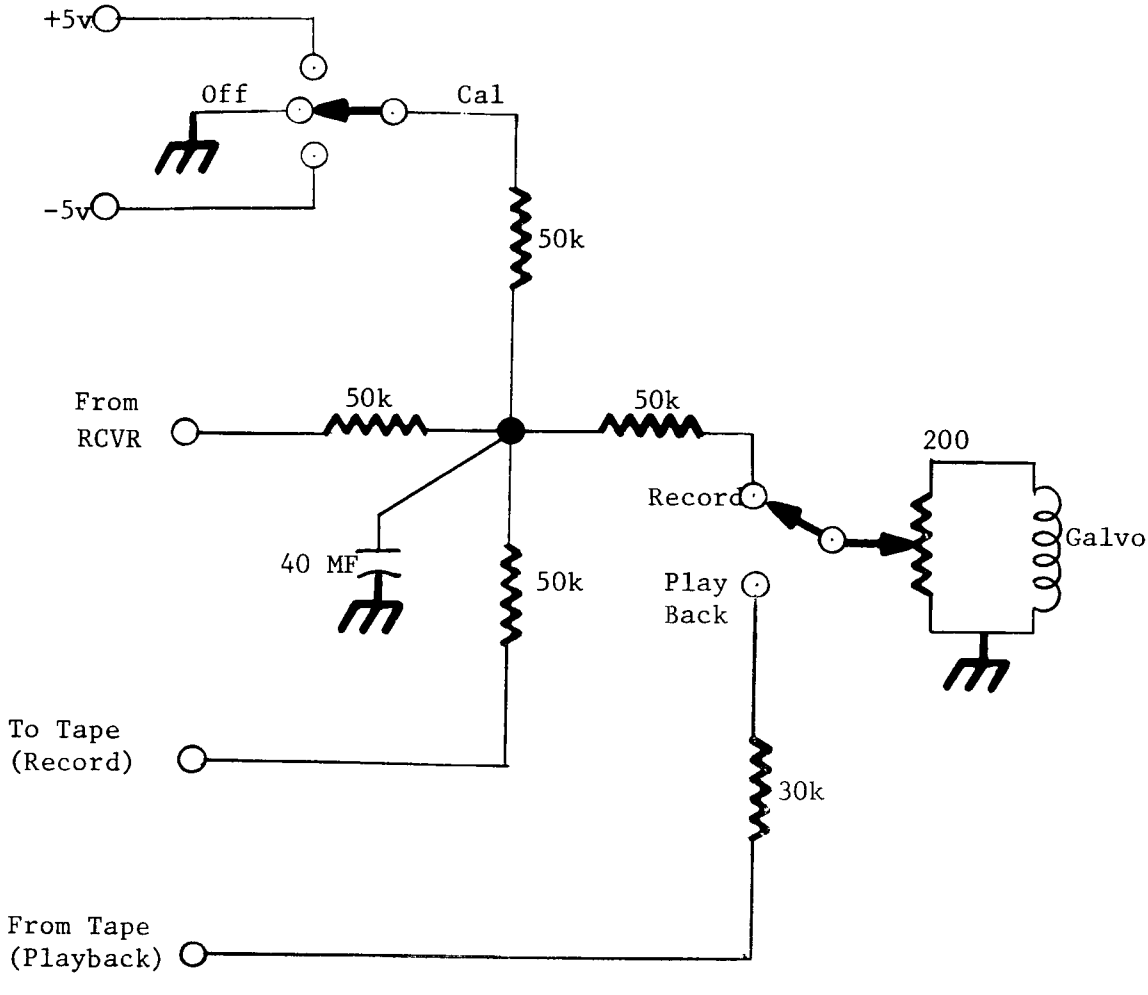

NOTE: Schematic typical for each of 16 channels

Fig. 3. Instrumentation panel

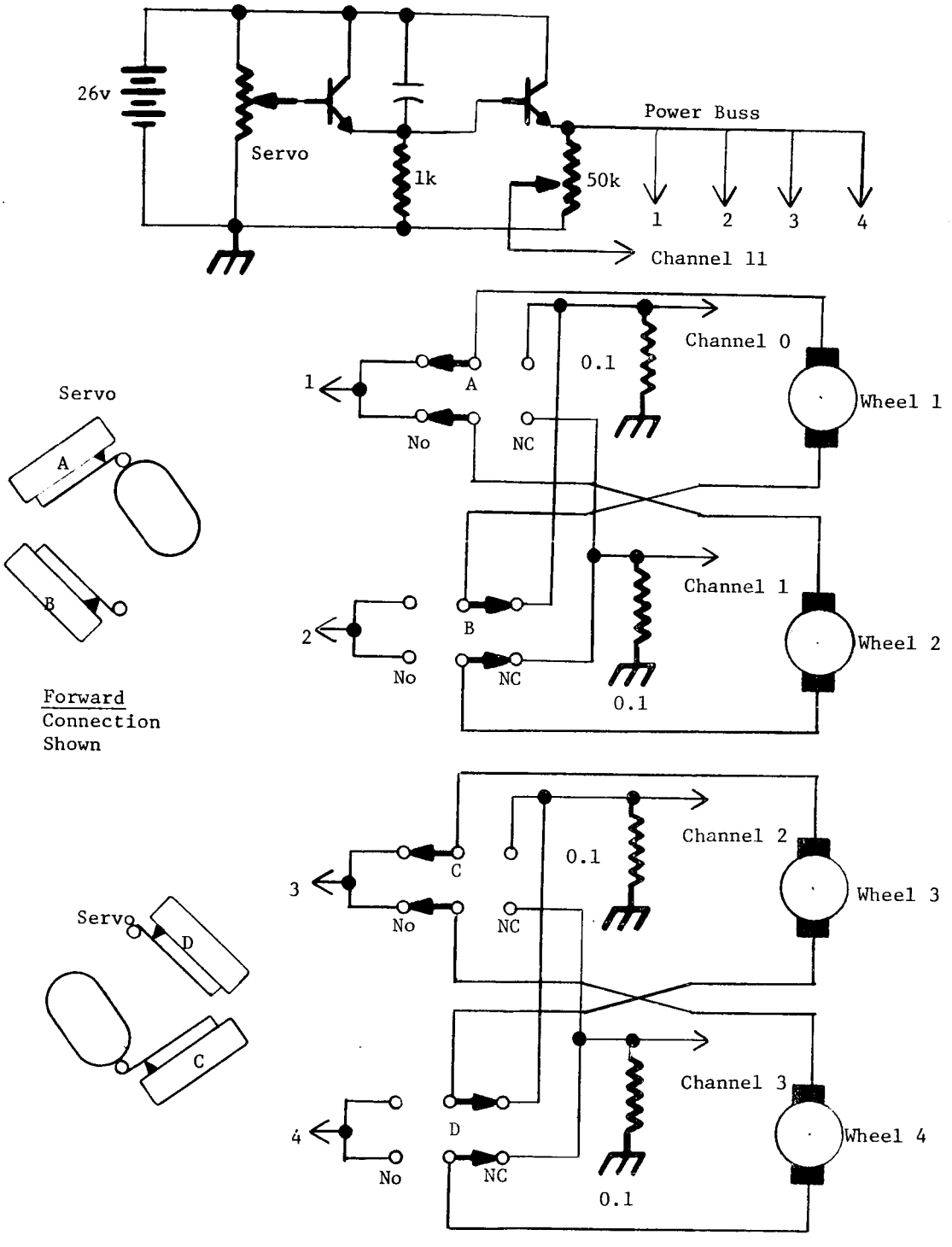

Fig. 4. Circuitry for drive motors

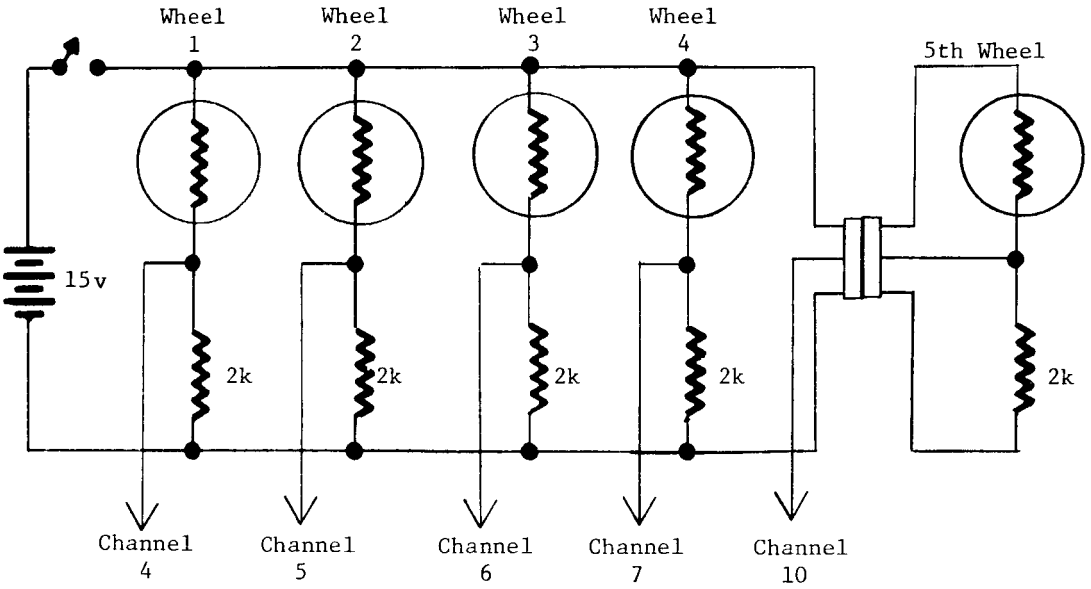

Light-Sensitive Resistors: Dark, 100k
Light, 20k

Fig. 5. Circuitry for determining wheel speed

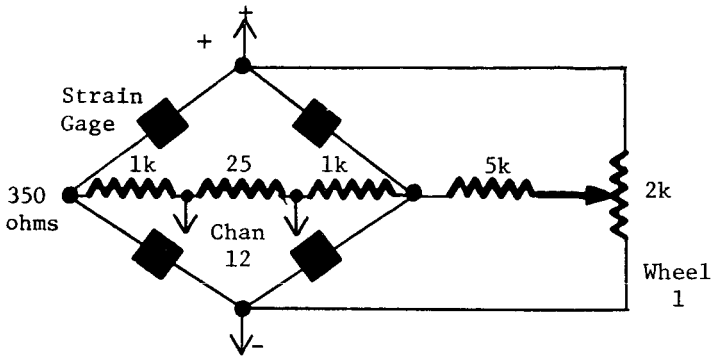

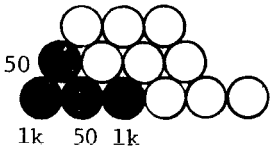

NOTE: 50 ohm resistors in parallel.

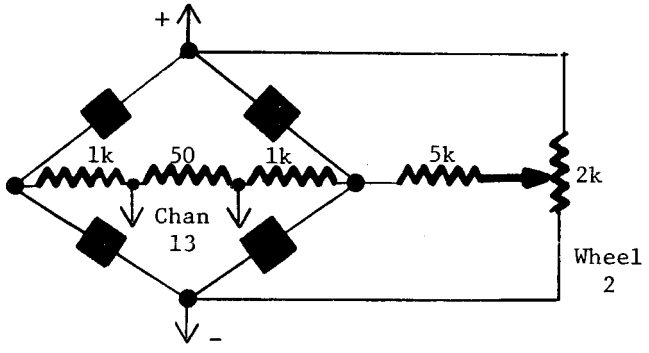

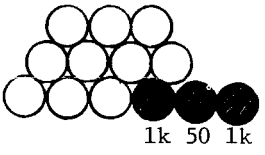

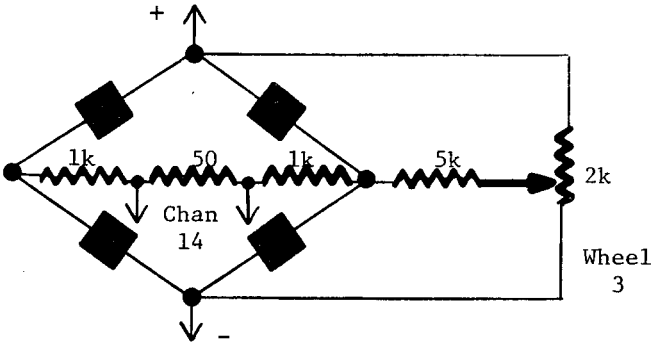

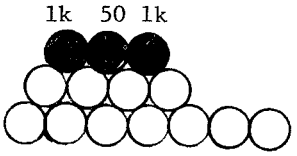

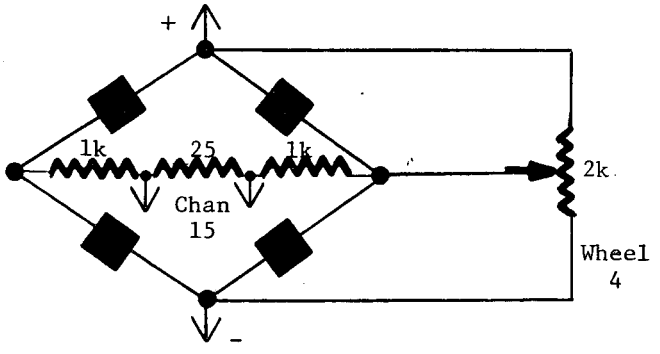

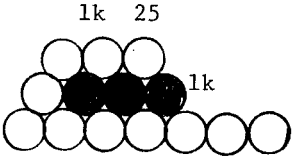

Position of sensitivity resistor in resistor pile located on vehicle

Fig. 6. Strain gages

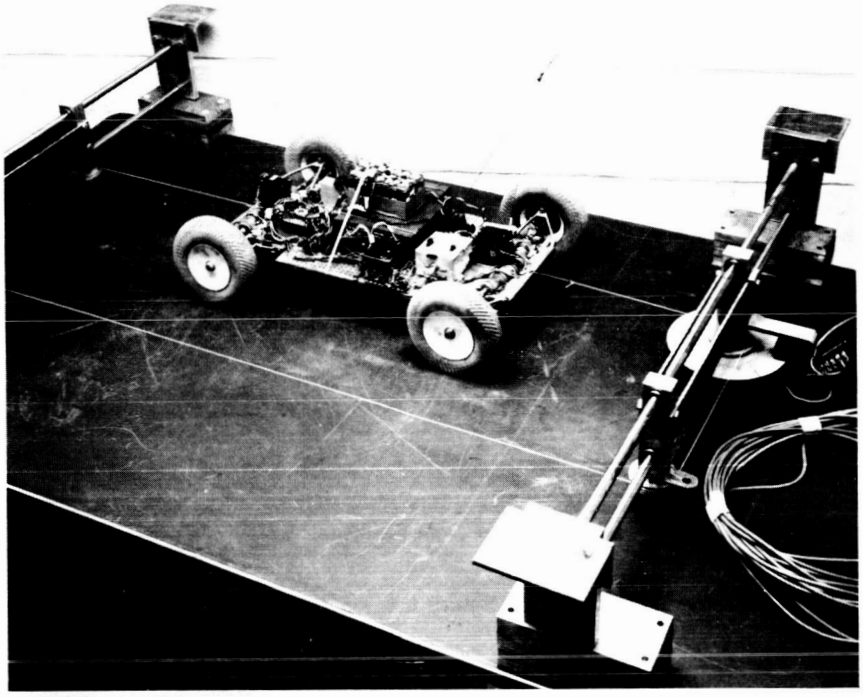

a. String-payout device for straight-line runs

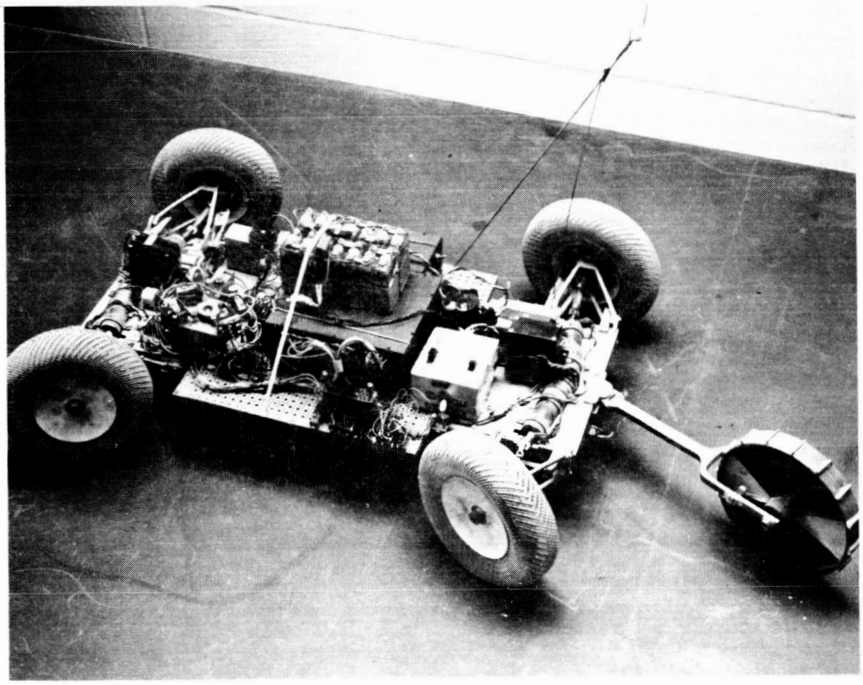

b. Fifth-wheel device for maneuvered runs

Fig. 7. Devices for measuring vehicle speed and elapsed time

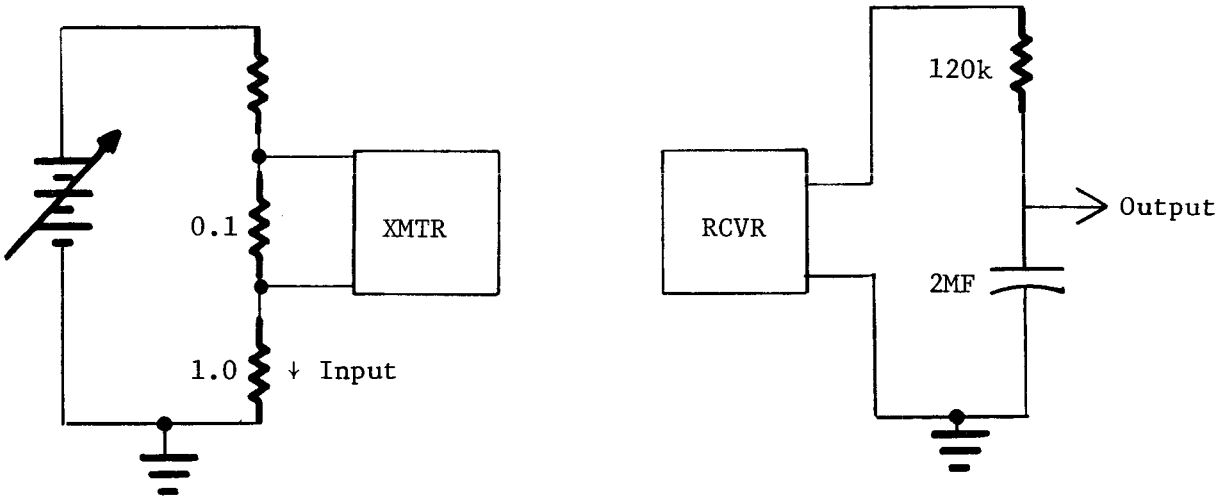

Fig. 8. Current calibration

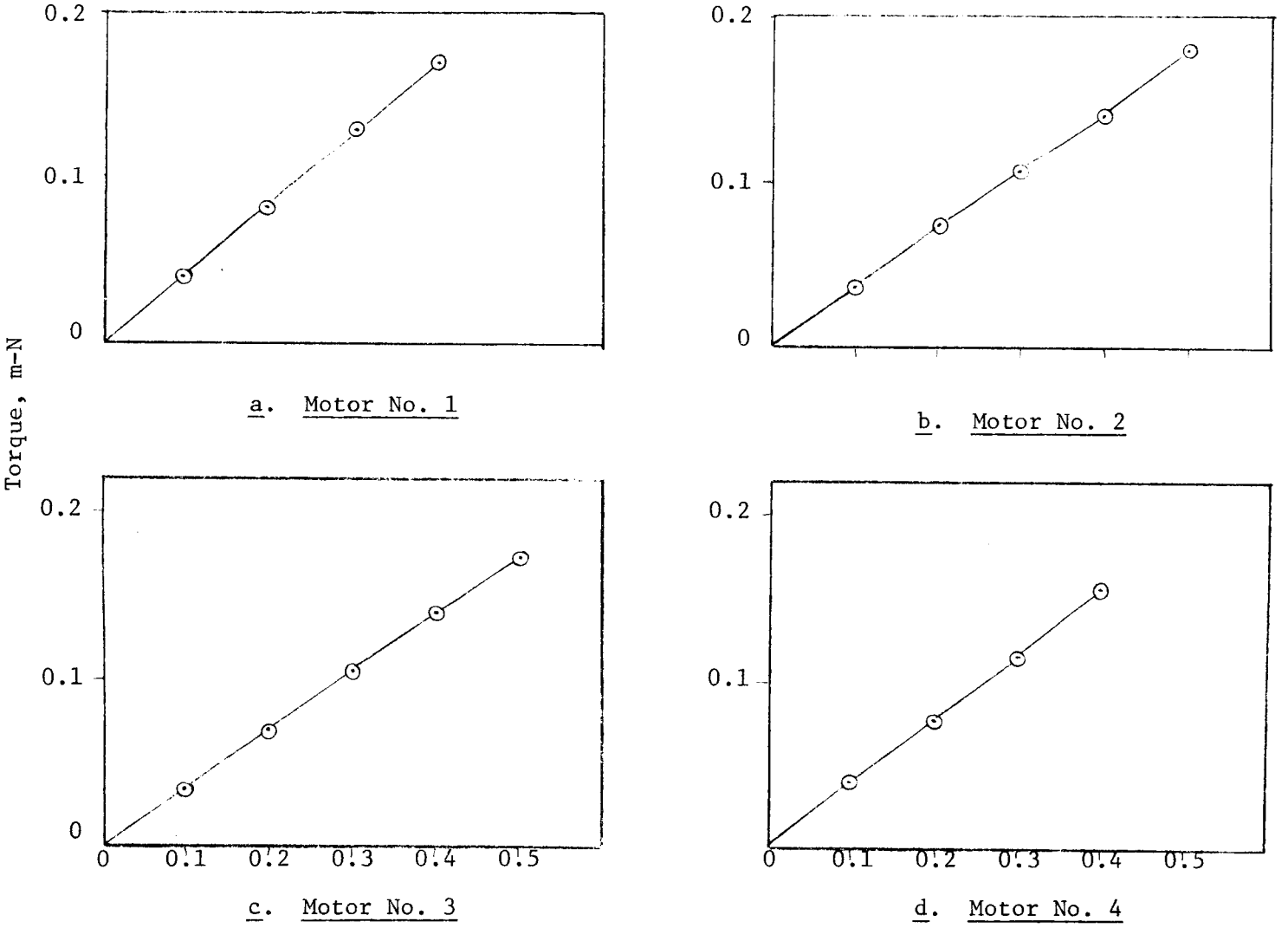

Fig. 9. Calibration of torque by measuring motor current

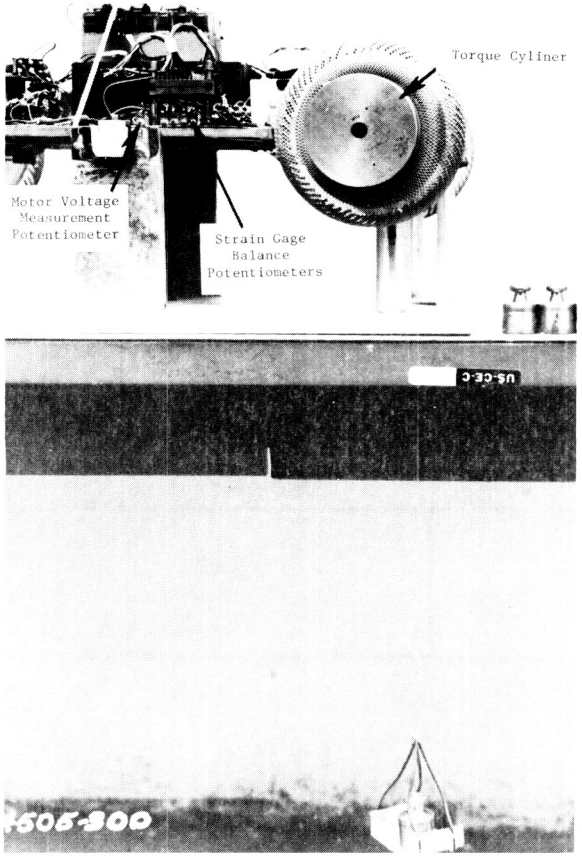

a

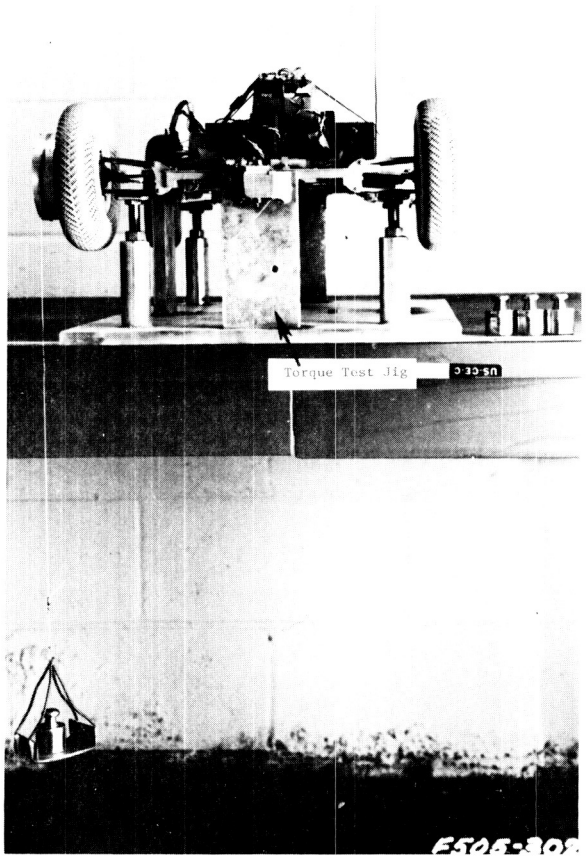

b

Fig. 10. Torque calibration setup

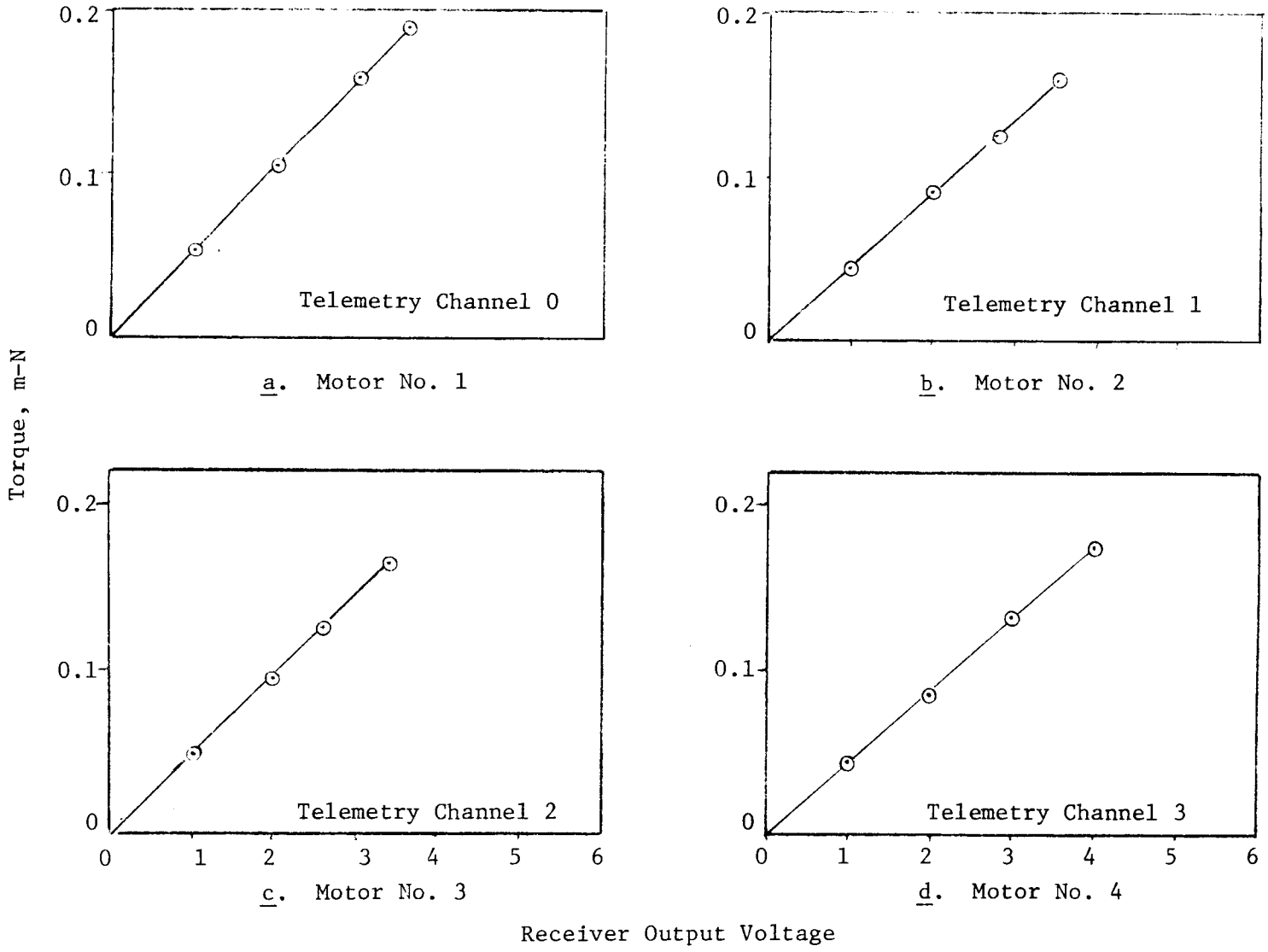

Fig. 11. Calibration of torque by telemetering voltage

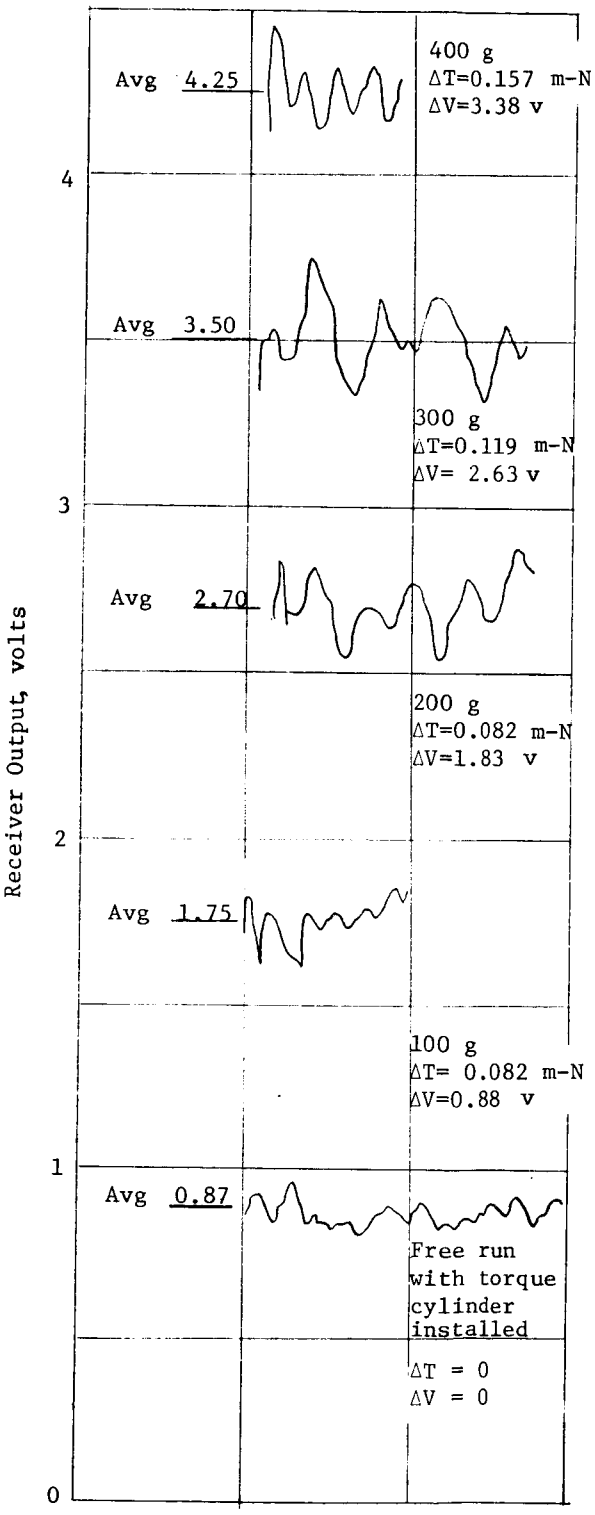

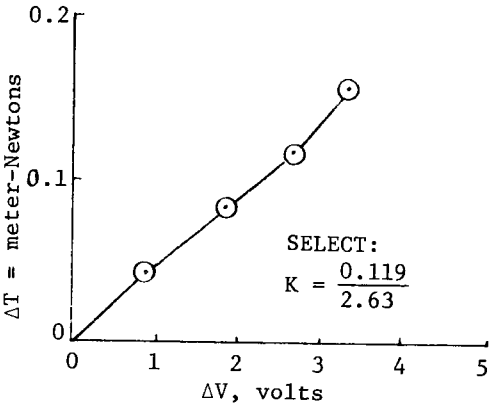

$T_0 + \Delta T = K(V_0 + \Delta V)$

Select K from graph of ΔT versus ΔV

Weight basket: 20.7 g
Torque cylinder radius: 3.81 cm

Fig. 12. Sample torque calibration

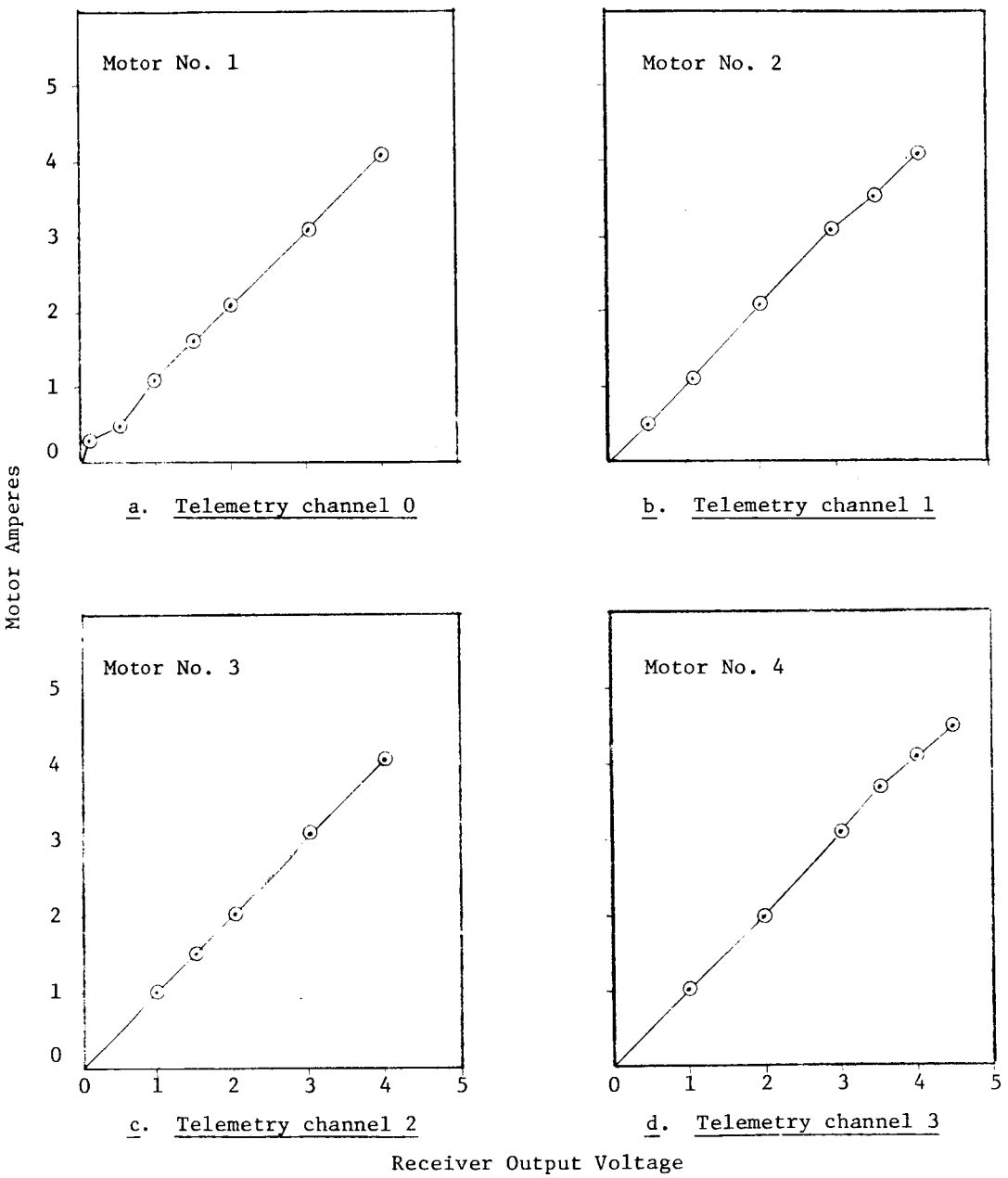

a. Telemetry channel 0

b. Telemetry channel 1

c. Telemetry channel 2

d. Telemetry channel 3

Fig. 13. Calibration of motor currents

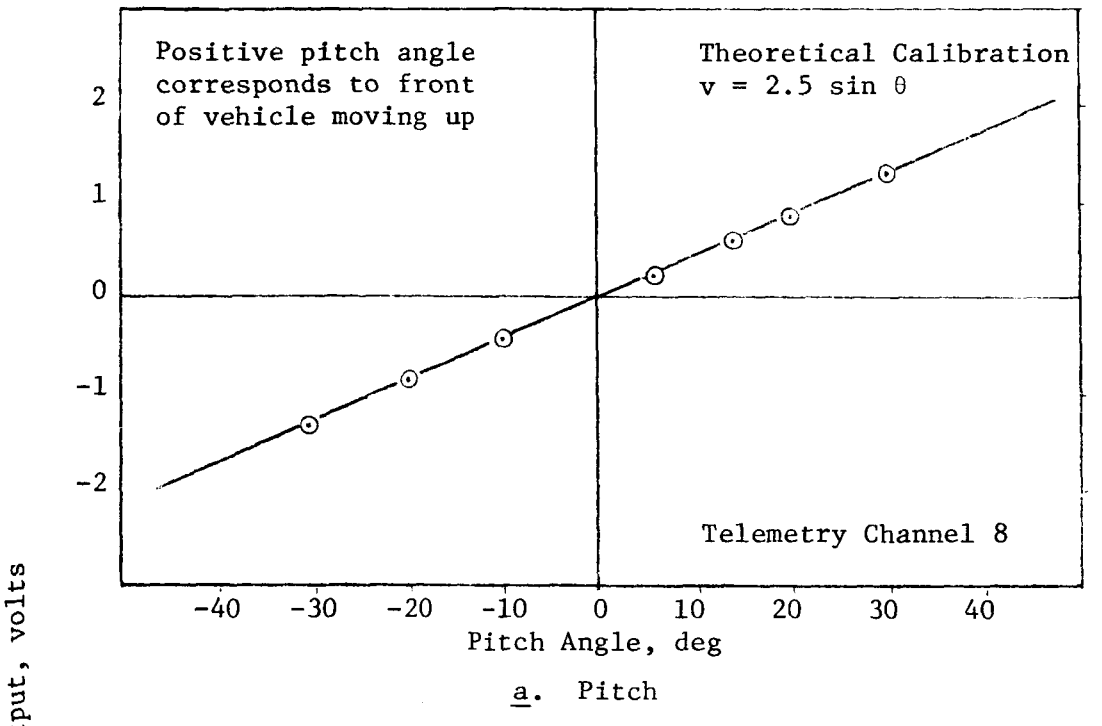

a. Pitch

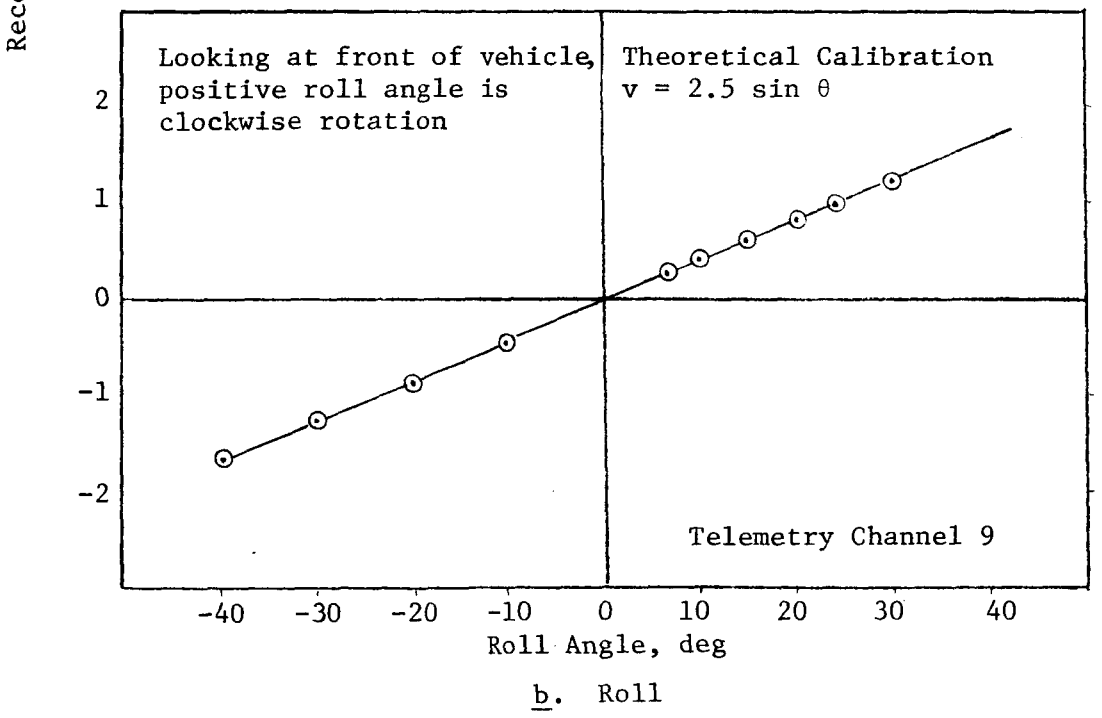

b. Roll

Fig. 14. Calibration of vehicle attitude

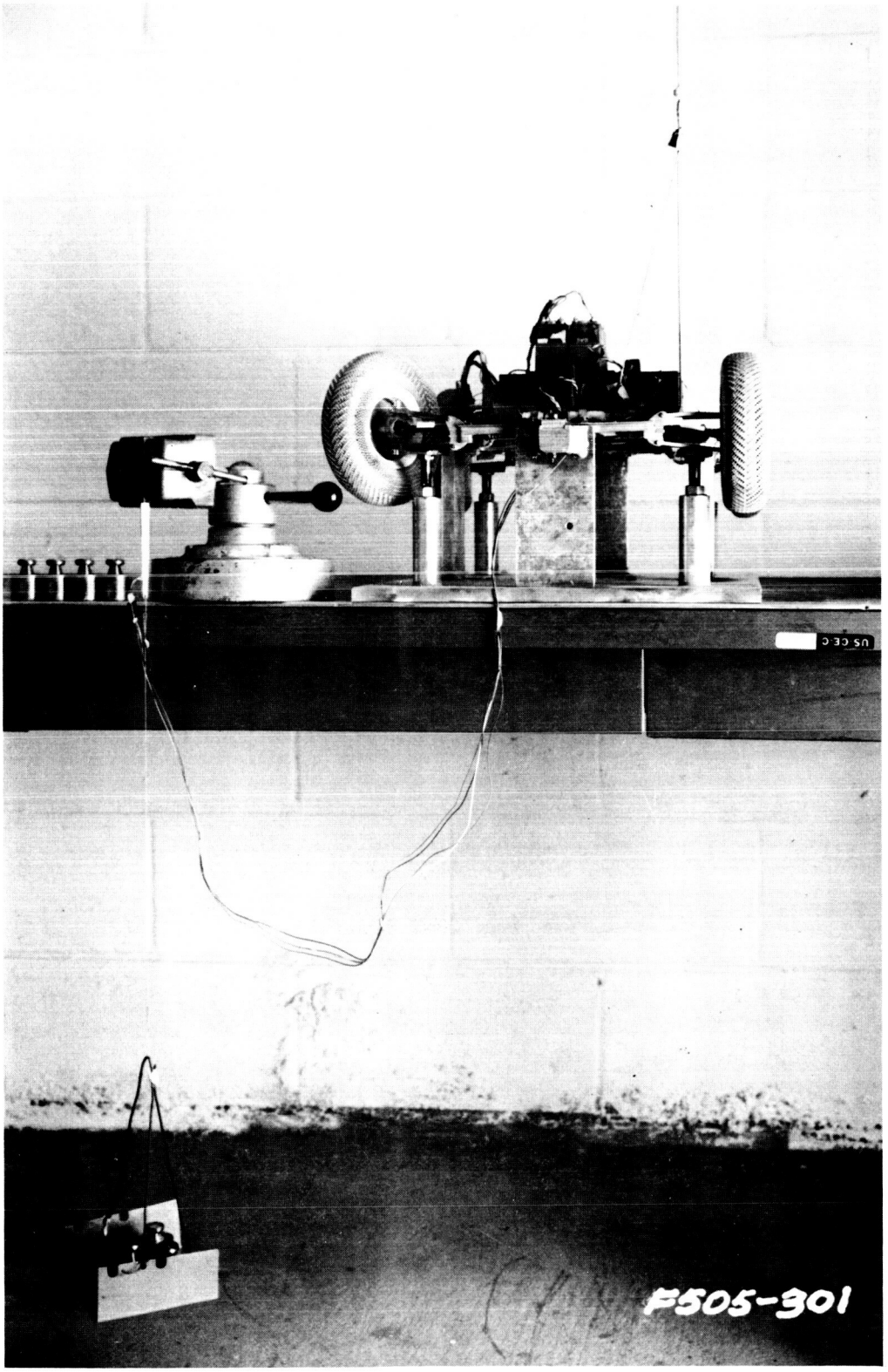

Fig. 15. Steering force calibration setup

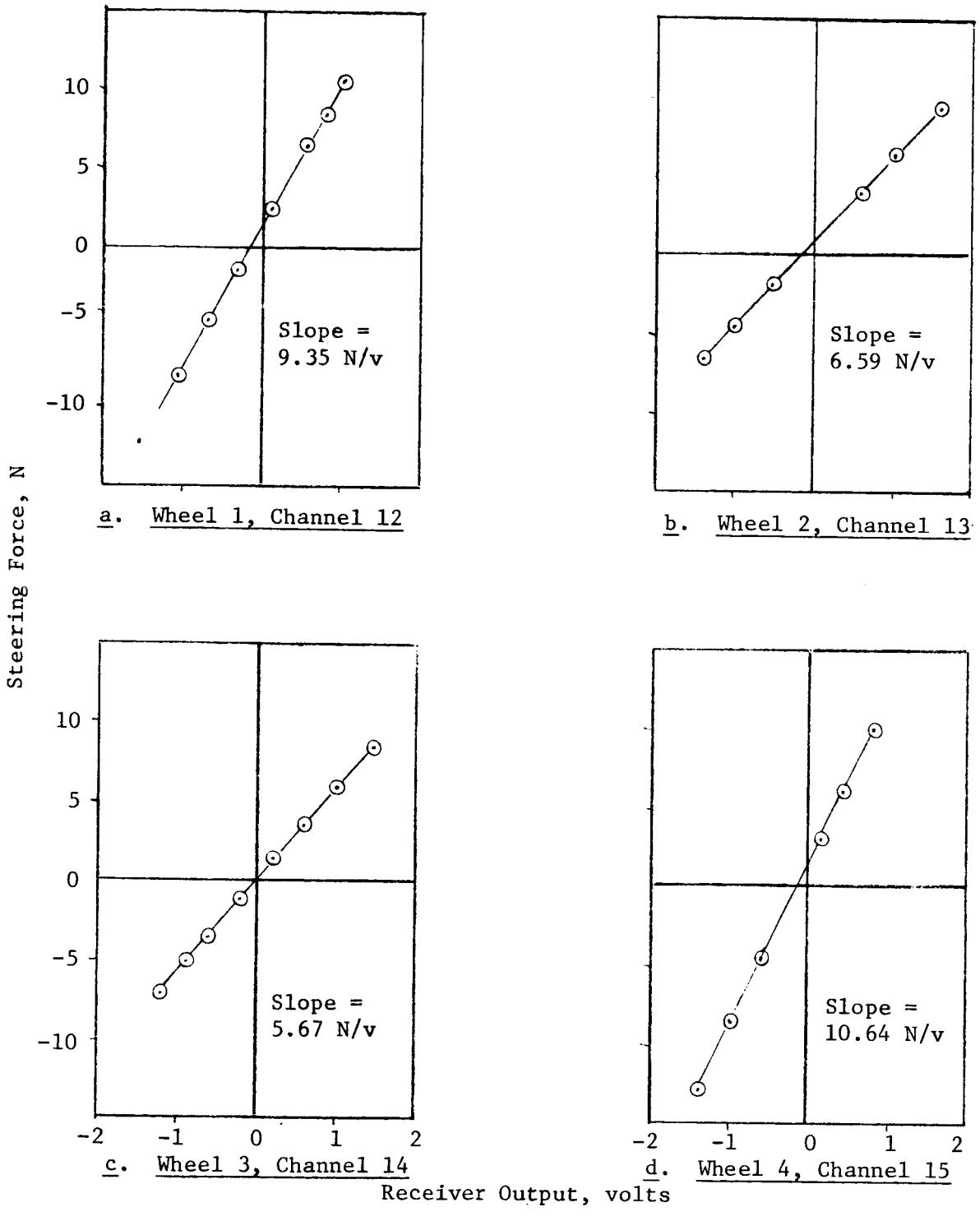

Fig. 16. Calibration of steering force

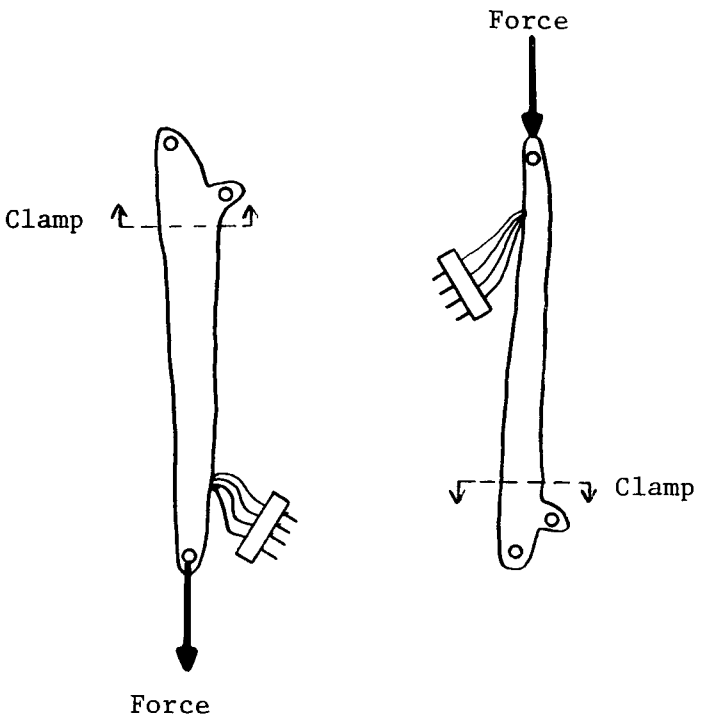

Fig. 17. Steering lines

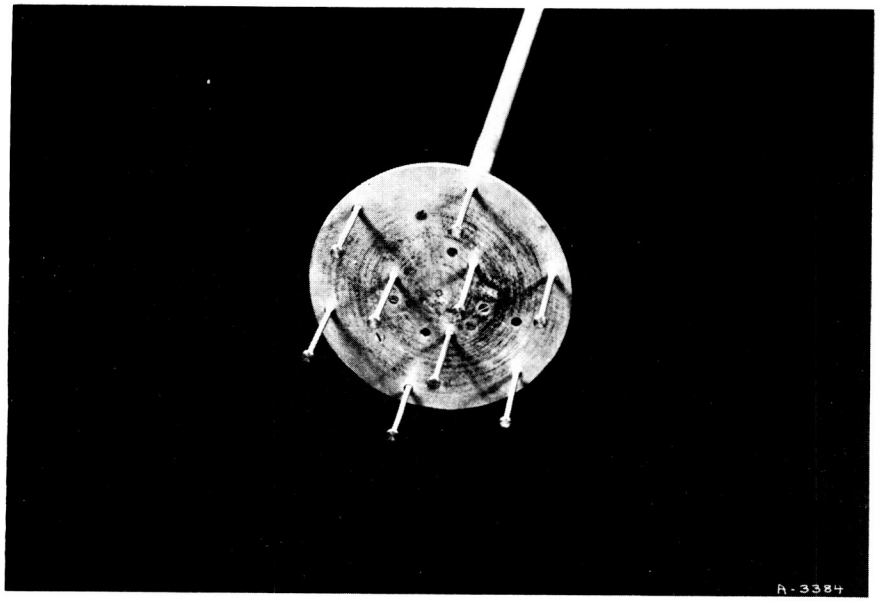

a. Bottom view

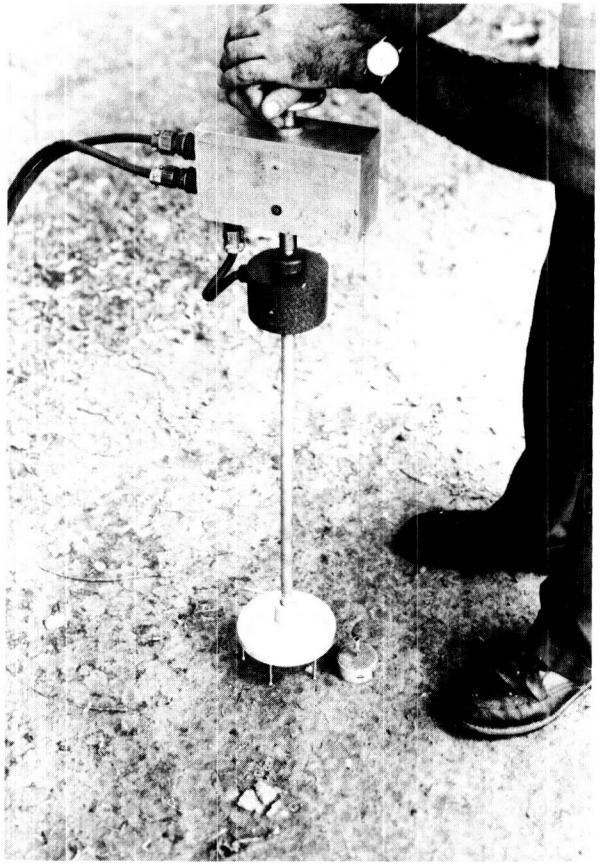

b. In use

Fig. 18. Multi-probe penetrometer

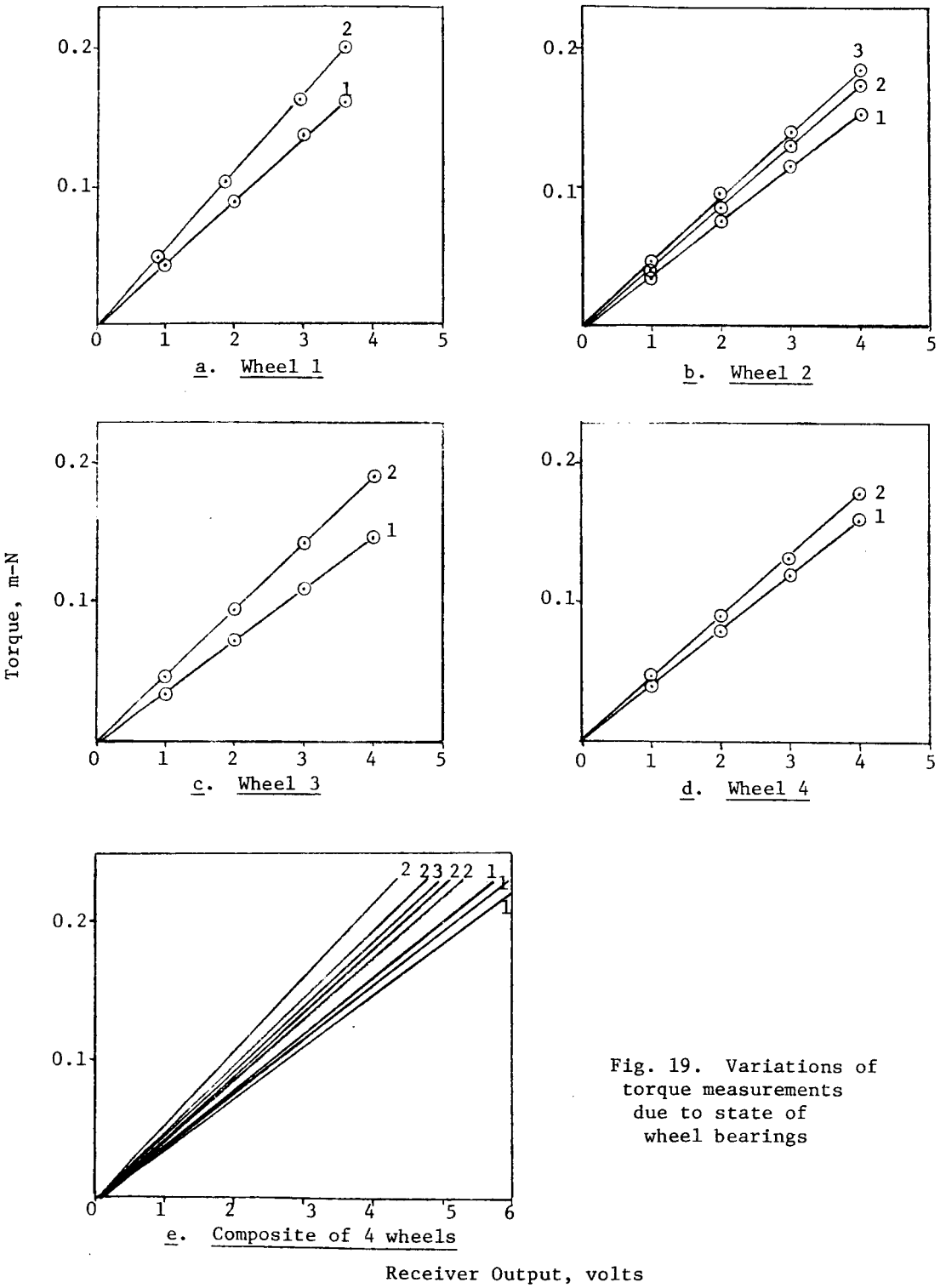

Fig. 19. Variations of torque measurements due to state of wheel bearings

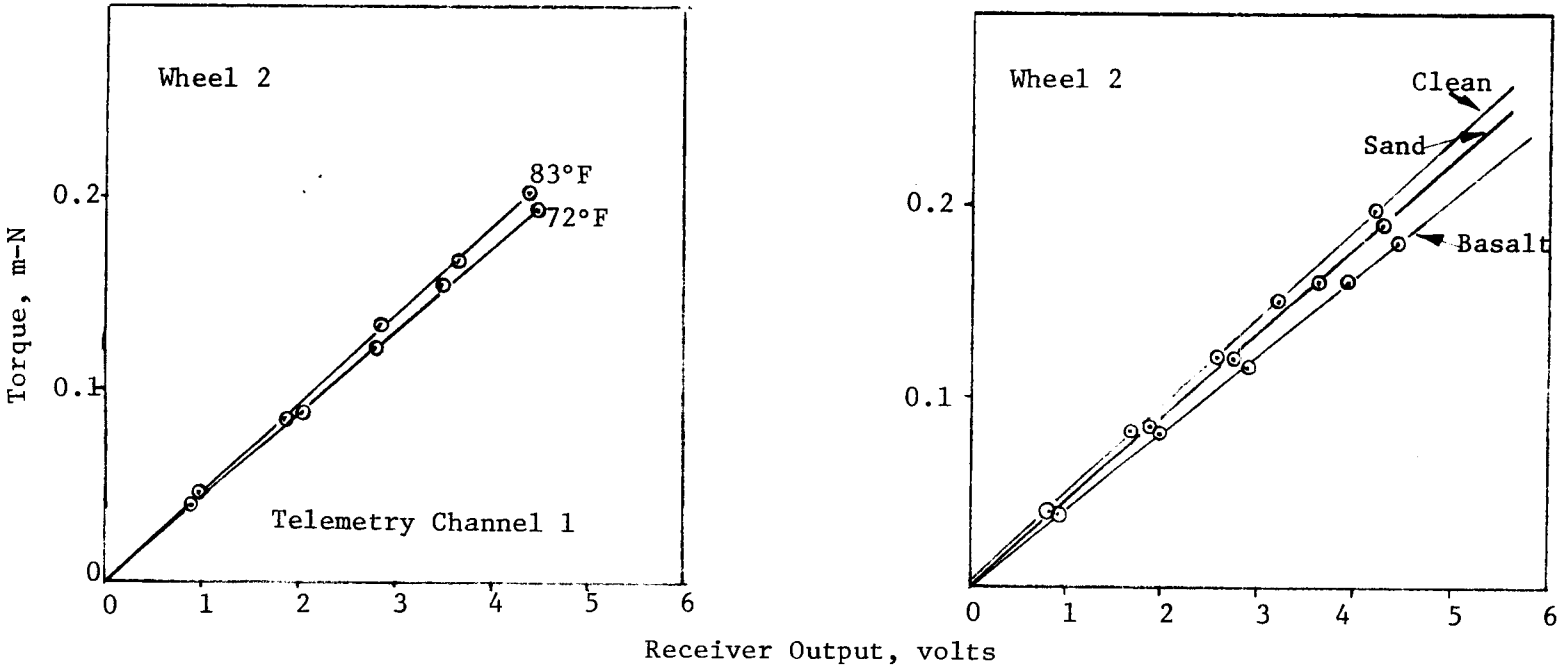

a. Temperature

b. Dust Environment

Fig. 20. Variations of torque measurements due to temperature and dust environment

APPENDIX A: FACTORS BEARING ON THE DESIGN OF THE SCALE-MODEL LRV

Dimensional Analysis

1. With respect to the following variables

m = mass	G = cone index gradient
p = soil mass density	V = vehicle speed
W = weight or load	g = acceleration of gravity
d = wheel diameter or any linear dimension	B = damping constant
	K = spring constant
c = soil cohesion	T = time

and the following assumptions (where "m" means "model on earth" and "p" means "prototype on moon")

$g_m = 6\ g_p$	$c_m = c_p$
$d_p = 6\ d_m$	$\rho_m = \rho_p$
$W_p = 36\ W_m$	$m_p = 216\ m_m$
$V_p = V_m$	$K_p = 6\ K_m$
$G_m = 6\ G_p$ (no cohesion)	$B_p = 36\ B_m$

the following dimensionless ratios are equivalent for the model on the earth and the prototype on the moon:

$\frac{W}{cd^2}$ (surface force numeric)

$\frac{W}{\rho g d^3}$ (body force numeric)

$\frac{W}{Gd^3}$ (sand loading numeric)*

$\frac{V^2}{gd}$ (Froude number)**

$\frac{mV^2}{Kd^2}$ (ratio of inertia to spring forces)

$\frac{mV}{Bd}$ (ratio of inertia to damping forces)

2. In addition, the sand mobility number*

$$\frac{G(bd)^{3/2}}{W} \cdot \frac{\delta}{h}$$

where

b = tire width

δ = tire deflection

h = tire section height

is also invariant between model and prototype.

3. For slight cohesion the assumption $G_m = 6\ G_p$ is no longer true,† and distortion occurs with respect to the sand loading numeric. However, distortion-free data may still be obtained with respect to the sand mobility number by controlling the ratio (δ/W) so that $\left(G\frac{\delta}{W}\right)_m = 36\left(\frac{G\delta}{W}\right)_p$

---

* D. R. Freitag, "A Dimensional Analysis of the Performance of Pneumatic Tires on Soft Soils," Technical Report No. 3-688, Aug 1965, U. S Army Engineer Waterways Experiment Station, CE, Vicksburg, Miss.

** D. Schuring, "Scale Model Testing of Land Vehicles in a Simulated Low Gravity Field," Paper No. 660148 presented at SAE Automotive Engineering Congress, Jan 1966, Detroit, Mich.

† N. C. Costes, private communication, 1971, George C. Marshall Space Flight Center, National Aeronautics and Space Administration, Huntsville, Ala.

4. The ratio VT/d can be kept constant between model and prototype by having $6\ T_m = T_p$. This suggests that frequencies are related by $f_m = 6\ f_p$.

5. Substantial agreement with this result has been obtained with drop tests of the LRV scale model, showing prominent frequencies of about 3 cyc/sec (see fig. A1), and field data from the prototype LRV showing frequencies of 0.5 to 0.33 cyc/sec.*

6. Because maneuvering is an important mode of operation of a free-running scale-model vehicle, it is pertinent to ask how the stability against overturn of the model relates to that of the prototype. An approximate analysis, with wheel and suspension deflections neglected, can be carried out as follows: In fig. A2, centrifugal force F acts horizontally through the center of gravity of a vehicle turning with radius R at speed V. When overturn is incipient, the sum of moments about point A is zero, or

$$Fd_1 = Wd_2$$

where d_1 is the lever arm of F about A, and d_2 is the lever arm of the vehicle weight W about A. But

$$F = \frac{mV^2}{R}$$

and

$$W = mg$$

or

$$\frac{mV^2}{R}d_1 = mgd_2$$

---

* Costes, op. cit., page A2.

A dimensionless form of this equation can be written as

$$\frac{gd_2R}{V^2d_1} = 1$$

Model and prototype should be related by

$$\left(\frac{gd_2R}{V^2d_1}\right)_m = \left(\frac{gd_2R}{V^2d_1}\right)_p$$

When the relations given earlier connecting g, V, and the linear dimensions are inserted into this expression, the equality is found to hold. Thus, the scaling conventions already selected to keep the foregoing numerics invariant between model and prototype are very likely satisfactory for studying overturn problems also.

Mechanical Considerations

7. When the scaling of linear dimensions and loads had been determined, problems of fabrication could be addressed. Materials were selected so that the combined weight of vehicle, radio control, and instrumentation would correspond to the scaled lunar prototype load. The vehicle was constructed almost entirely of magnesium. The wheels were constructed of a nylon mesh of proper rigidity to produce a scaled load-deflection characteristic.

8. With the size and weight of the model and the wheel loading and suspension travel characteristics properly accounted for, the remainder of the design process made no appeal to scaling laws. Specifically, there was no similarity between model and prototype electrical propulsion systems or vehicle body superstructure. With respect to the propulsion

system, the principal problem was to find motors and gear boxes capable of delivering sufficient torque to propel the model in soft soil and yet be small enough to mount conveniently on the model. There was no possibility of devising a scaled-down system with the motors mounted in the wheels. The motors were mounted on the vehicle body and linked to the wheels through double universal joints and splined shafts. This arrangement, for which no reasonable alternative could be found, had considerable frictional loss in the composite drive shaft, as indicated by the unsteady components of motor current shown in fig. 12.

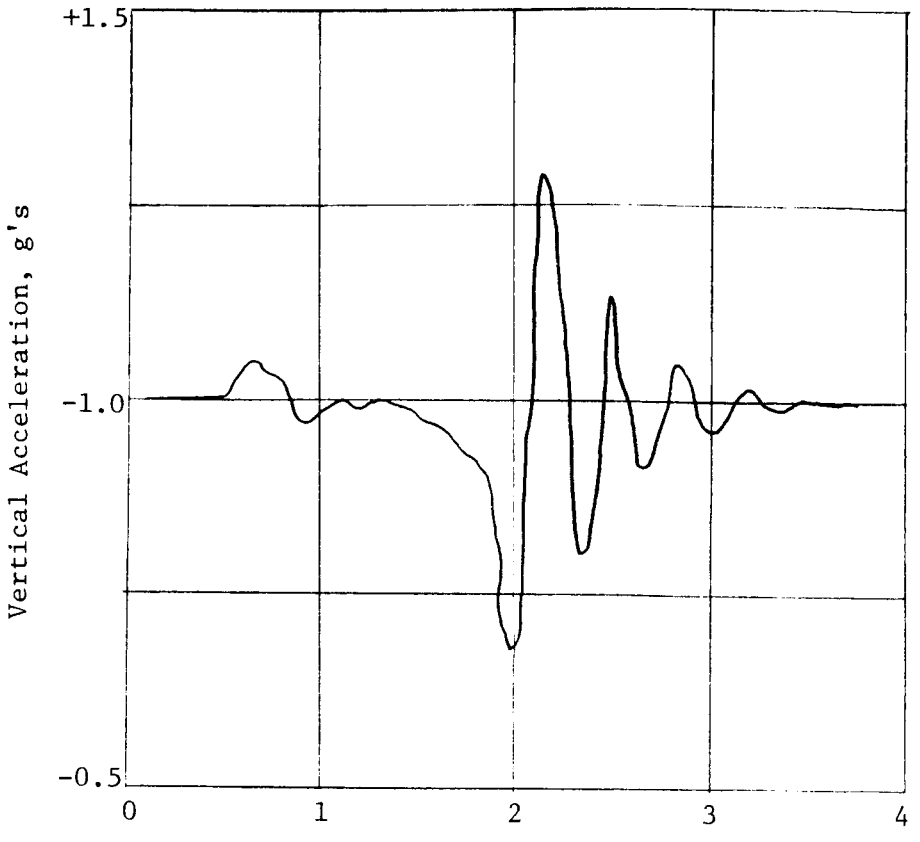

Fig. A1. Typical outcome of scale-model drop test

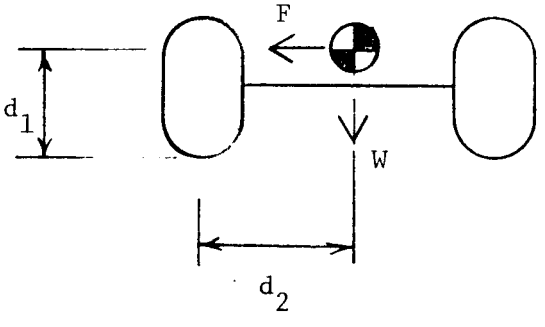

Fig. A2. Overturn force balance

Unclassified

Security Classification

DOCUMENT CONTROL DATA - R & D

(Security classification of title, body of abstract and indexing annotation must be entered when the overall report is classified)

1. ORIGINATING ACTIVITY *(Corporate author)*
U. S. Army Engineer Waterways Experiment Station
Vicksburg, Mississippi

2a. REPORT SECURITY CLASSIFICATION
Unclassified

2b. GROUP

3. REPORT TITLE
OPERATIONS AND MAINTENANCE MANUAL FOR A SCALE-MODEL LUNAR ROVING VEHICLE

4. DESCRIPTIVE NOTES *(Type of report and inclusive dates)*
Final report

5. AUTHOR(S) *(First name, middle initial, last name)*
Allen S. Lessem

6. REPORT DATE	7a. TOTAL NO. OF PAGES	7b. NO. OF REFS
April 1972	59	5

8a. CONTRACT OR GRANT NO.	9a. ORIGINATOR'S REPORT NUMBER(S)
b. PROJECT NO.	Miscellaneous Paper M-72-3
c. NASA - Defense Purchase Request No. H-72026A	9b. OTHER REPORT NO(S) *(Any other numbers that may be assigned this report)*
d.	

10. DISTRIBUTION STATEMENT
Approved for public release; distribution unlimited.

11. SUPPLEMENTARY NOTES	12. SPONSORING MILITARY ACTIVITY
	George C. Marshall Space Flight Center National Aeronautics and Space Administration, Huntsville, Alabama

13. ABSTRACT

A one-sixth scale model of the Lunar Roving Vehicle used in the Apollo 15 mission was built and instrumented to conduct model studies of vehicle mobility. The model was free running under radio control and was equipped with a lightweight telemetry transmitter that allowed 16 channels of data to be gathered simultaneously. String payout and fifth-wheel devices were developed to measure vehicle velocity. Other real-time measurements included wheel torque, wheel speed, center-of-gravity accelerations, and steering forces. Calibration, operations, and maintenance procedures were worked out. Details of the development of the instrumentation, its maintenance, some of the problems encountered, etc., are recorded in this report to serve as a preliminary operations and maintenance manual for this specific model. In addition, information regarding soil processing and testing that may be useful to NASA personnel planning mobility research with the model in soil is furnished.

DD FORM 1 NOV 68 1473 REPLACES DD FORM 1473, 1 JAN 64, WHICH IS OBSOLETE FOR ARMY USE.

Unclassified

Security Classification

14. KEY WORDS	LINK A		LINK B		LINK C	
	ROLE	WT	ROLE	WT	ROLE	WT
Lunar roving vehicles						
Lunar soils						
Models						